Preprint typeset in JHEP style - HYPER VERSION IFT-UAM/CSIC-12-122

The health of SUSY after the Higgs discovery and the XENON100 data

Maria Eugenia Cabrera

University of Amsterdam
Institute of Theoretical Physics
GRAPPA

J. Alberto Casas

Instituto de Física Teórica, IFT-UAM/CSIC
U.A.M., Cantoblanco,
28049 Madrid, Spain

Roberto Ruiz de Austri

Instituto de Física Corpuscular, IFIC-UV/CSIC
Valencia, Spain

arXiv:1212.4821v1 [hep-ph] 19 Dec 2012

Abstract:
We analyze the implications for the status and prospects of supersymmetry of the Higgs discovery and the last XENON data. We focus mainly, but not only, on the CMSSM and NUHM models. Using a Bayesian approach we determine the distribution of probability in the parameter space of these scenarios. This shows that, most probably, they are now beyond the LHC reach . This negative chances increase further (at more than 95% c.l.) if one includes dark matter constraints in the analysis, in particular the last XENON100 data. However, the models would be probed completely by XENON1T. The mass of the LSP neutralino gets essentially fixed around 1 TeV. We do not incorporate ad hoc measures of the fine-tuning to penalize unnatural possibilities: such penalization arises automatically from the careful Bayesian analysis itself, and allows to scan the whole parameter space. In this way, we can explain and resolve the apparent discrepancies between the previous results in the literature. Although SUSY has become hard to detect at LHC, this does not necessarily mean that is very fine-tuned. We use Bayesian techniques to show the experimental Higgs mass is at $\sim 2\ \sigma$ off the supersymmetric expectation. This is substantial but not dramatic. Although the CMSSM or the NUHM are unlikely to show up at the LHC, they are still interesting and plausible models after the Higgs observation; and, if they are true, the chances of discovering them in future dark matter experiments are quite high.

Keywords: Physics Beyond Standard Model, Supersymmetry Phenomenology, Higgs Physics, LHC Physics, Dark Matter Searches.

Contents

1. Introduction 1

2. Set up 3

2.1 The Bayesian approach 4

2.2 Model-independent incorporation of naturalness criteria in the MSSM 5

2.3 Priors in the initial parameters 7

3. Physical observables and computational methods used in the analysis 9

4. Results for the CMSSM 12

4.1 Results with no dark matter constraints 13

4.2 Incorporation of dark matter 17

4.3 g-2 24

5. NUHM 26

6. Can still SUSY be natural? The impact of the Higgs discovery in the naturalness of SUSY 27

7. Comparison with previous literature 33

8. Conclusions 35

A. Focus-Point behavior in the CMSSM and the NUHM 36

1. Introduction

The ATLAS and CMS collaborations have reported [1, 2] the strong evidence evidence of a Standard Model (SM) -like Higgs boson with $m_h \sim 126$ GeV. According to the most recent analysis presented in the Kyoto conference [3, 4], which combines the $\sqrt{s} = 7$ TeV (L=5.0 fb^{-1}) and $\sqrt{s} = 8$ TeV (L=12.1 fb^{-1}) data, the "Higgs-boson" mass is

$$\begin{aligned} m_h &= 126.0 \pm 0.4\ (\text{stat}) \ \pm 0.4\ (\text{syst})\ \text{GeV} \quad (\text{ATLAS}) \\ m_h &= 125.7 \pm 0.4\ (\text{stat}) \ \pm 0.4\ (\text{syst})\ \text{GeV} \quad (\text{CMS})\ . \end{aligned} \tag{1.1}$$

Adding the statistical and systematic uncertainties in quadrature, and combining further the ATLAS and CMS results, using the principle of maximum likelihood, one finds the following central value and uncertainty

$$m_h \;=\; 125.85 \pm 0.4 \quad . \tag{1.2}$$

Beyond the crucial importance of this discovery by itself, this result has far-reaching consequences for well-motivated candidates for physics beyond the SM, such as Supersymmetry (SUSY), and in particular the Minimal Supersymmetric Standard Model (MSSM).

Many works have explored these implications from different points of view, often relying on popular versions of the MSSM, such as the constrained MSSM (CMSSM) or the (slightly less restrictive) non-universal Higgs masses model (NUHM). In addition, some analyses incorporate as well the recent XENON100 constraints on fermionic dark matter [5, 6, 7, 8, 9, 10, 11]. Roughly speaking, the MSSM is in trouble, since a $\sim 125 - 126$ GeV Higgs generically requires rather large SUSY masses, which is in tension with the naturalness of the electroweak breaking at the correct scale. A big portion of the previously-acceptable CMSSM and NUHM parameter-space becomes excluded. Some of these explorations present the results in the form of scatter plots, which illustrate the acceptable regions in slides of the parameter space, see e.g. [10]. While these analyses certainly reflect the situation, it is more difficult to tell from them the degree of tension of the CMSSM and the NUHM (or the general MSSM) with the experimental result $m_h \simeq 126$ GeV or what is the relative probability of the various regions of the associated parameter-space.

There are two main strategies to attack these questions: the frequentist and the Bayesian approaches. The frequentist one is based on the analysis of the likelihood function in the parameter space: one performs a scan of the parameter space, evaluating the likelihood based on the χ^2. This leads to zones of estimated probability (inside contours of constant χ^2) around the best fit points. In doing so, the unplotted variables are optimized to obtain the best χ^2. A nice feature of the frequentist approach is that it does not require to establish a prior to analize the parameter space. Essentially, it corresponds to a search of the points with best likelihood, and therefore gives relevant information about the goodness of different regions of the parameter space. However, a frequentist approach does not give necessarily the fair probability-map of the parameter space of a model. This is obtained using a Bayesian approach.

As an example of this, let's take the notion of fine-tuning. Fine-tuning has to do with statistical weight and a frequentist analysis is based entirely on likelihood, i.e. the ability to reproduce the experiment, and thus cannot "see" the fine-tuning. E.g. a point (o a region) in the parameter space can present an optimal likelihood, but only after an extreme tuning of the unplotted parameters. This feature makes this point extremely unplausible (even if it is capable to reproduce the experimental data), but this does not affect its privileged condition in a frequentist approach. On the other hand, a correct Bayesian analysis incorporates automatically (without any ad hoc consideration) a penalization of the fine-tuned regions, since they have little statistical weight.

Therefore the Bayesian approach offers a representative diagnosis of the health of a theoretical scenario and the future prospects. The main goal of this paper is to perform such Bayesian diagnosis in full detail, incorporating the impact of a possible Higgs at $\simeq 126$ GeV, as well as the last XENON100 dark-matter constraints and other recent experimental data. We will also incorporate significant improvements over previous Bayesian explorations. They will allow us to avoid the arbitrariness associated to the choice of the ranges where the parameters live. We will show that this ambiguity is the origin of important apparent discrepancies between previous literature. From the analysis we obtain the most probable regions in the CMSSM and NUHM parameter space and study the capacity of the LHC and XENON of probing those regions in the future.

Using Bayesian techniques, we will also explore in more general terms how the Higgs discovery affects the naturalness of SUSY, quantifying the tension between $m_h \simeq 126$ GeV and the supersymmetric predictions.

In sect. 2 we establish our set up, reviewing the Bayesian approach and how it can be rigorously implemented in the context of the MSSM. We discuss also the choice of priors issue. In sect. 3 we list the observables used in the analysis in order to calculate the likelihood of the different points of the parameter space. We also expose the different codes and computational techniques used in the numerical calculations. Sect. 4 is devoted to the results for the CMSSM. We present them with and without dark matter constraints. We also distinguish between the possibility that the dark matter is purely supersymmetric or it has other components. We also quantify the discrepancy between present experimental data on $g-2$ and the Higgs mass in the supersymmetric framework. This quantifiable tension is the reason why we have chosen not to include $g-2$ data in the analysis until the theoretical situation becomes fully clarified. In sect. 5 we perform a similar analysis for the NUHM and present the results. In sect. 6 we study the issue of the naturalness of SUSY after the Higgs discovery, using Bayesian techniques. Sect. 7 is devoted to the comparison with previous literature on this subject and to discuss the reasons of the apparent discrepancies. The conclusions are presented in sect. 8. In addition we describe some meaningful theoretical aspects of the Focus-Point region in the CMSSM and the NUHM.

2. Set up

We will consider two versions of the minimal supersymmetric standard model (MSSM), namely the so-called constrained MSSM (CMSSM) and the non-universal Higgs masses model (NUHM). In the CMSSM the soft parameters are assumed universal at a high scale (M_X), where the supersymmetry (SUSY) breaking is transmitted to the observable sector, as happens e.g. in the gravity-mediated SUSY breaking scenario. The CMSSM parameter-space is then defined by the following parameters:

$$\{\theta_i\} \;=\; \{m_0, m_{1/2}, A, B, \mu, s\}\ . \tag{2.1}$$

Here m_0, $m_{1/2}$ and A are the universal scalar mass, gaugino mass and trilinear scalar coupling; B is the bilinear scalar coupling; μ is the usual Higgs mass term in the superpotential; and s stands for the SM-like parameters of the model, i.e. essentially gauge and Yukawa couplings. All these initial parameters are understood to be defined at M_X. The NUHM is defined by the same parameters as the CMSSM but allowing for a different scalar mass for the two Higgs doublets, m_H.

2.1 The Bayesian approach

The goal of the Bayesian approach is to generate a map of the relative probability of the different regions of the parameter space of the model under consideration (CMSSM and NUHM in our case), using all the available (theoretical and experimental) information. This is the so-called *posterior* or probability density function (pdf), $p(\theta_i|\text{data})$, where "data" stands for all the experimental information and θ_i represent the various parameters of the model. The posterior is given by the fundamental Bayesian relation

$$p(\theta_i|\text{data}) \;=\; p(\text{data}|\theta_i)\; p(\theta_i)\; \frac{1}{p(\text{data})}\;, \tag{2.2}$$

where $p(\text{data}|\theta_i)$ is the likelihood (sometimes denoted by $\mathcal{L}$), i.e. the probability density of measuring the given data for the chosen point in the parameter space (this is the quantity used in frequentist approaches); $p(\theta_i)$ is the prior, i.e. the "theoretical" probability density that we assign a priori to the point in the parameter space; and finally, $p(\text{data})$ is a normalization factor which plays no role unless one wishes to compare different classes of models, so for the moment it can be dropped from the previous formula. One can say that in eq. (2.2) the first factor (the likelihood) is objective, while the second (the prior) contains our prejudices about how the probability is distributed a priori in the parameter space, given all our previous knowledge about the model.

Ignoring the prior factor is not necessarily the most reasonable or "free of prejudices" attitude. Such procedure amounts to an implicit choice for the prior, namely a completely flat prior in the parameters. However, one needs some theoretical basis to establish, at least, the parameters whose prior can be reasonably taken as flat.

Besides, note that a choice for the allowed ranges of the various parameters is necessary in order to make statistical statements. Often one is interested in showing the probability density of one (or several) of the initial parameters, say $\theta_i,\ i = 1, ..., N_1$, but not in the others, $\theta_i,\ i = N_1 + 1, ..., N$. Then, one has to *marginalize* the latter, i.e. integrate in the parameter space:

$$p(\theta_i,\ i = 1, ..., N_1|\text{data}) \;=\; \int d\theta_{N_1+1}, ..., d\theta_N\; p(\theta_i,\ i = 1, ..., N|\text{data})\;. \tag{2.3}$$

This procedure is very useful and common to make predictions about the values of particularly interesting parameters. Now, in order to perform the marginalization, we need an input for the prior functions *and* for the range of allowed values of the parameters, which determines the range of the definite integration (2.3). A choice for these ingredients is therefore inescapable in trying to make Bayesian LHC forecasts.

In consequence, an important indicator of the reliability of the results of a Bayesian analysis is the dependence of the results on the choice of the prior and on the ranges established for the unknown parameters, something that is addressed in the present paper (and very seldom done).

2.2 Model-independent incorporation of naturalness criteria in the MSSM

The main motivation of low-energy SUSY is the nice implementation of the electroweak (EW) breaking, since the EW scale (or, equivalently, the Z mass) does not suffer from enormous (quadratic) radiative corrections that occur in the SM. Actually, in the MSSM the EW breaking occurs naturally in a substantial part of the parameter space. This success is greatly due to the SUSY radiative contributions to the Higgs potential. Of course, in our analysis, the points of the parameter space that do not have a correct EW breaking are to be discarded, as usual.

It is common lore that the parameters of the MSSM, $\{m_0, m_{1/2}, A, B, \mu\}$, should not be far from the experimental EW scale in order to avoid unnatural fine-tunings to obtain the correct size of the EW breaking. Previous Bayesian studies of the MSSM have attempted to incorporate this criterion by implementing some penalization of the fine-tuned regions or (more usually) by restricting the range of the soft parameters to $\lesssim$ few TeV. This is more or less reasonable, but makes the results dependent on the actual ranges considered (although normally such test is not presented).

On the other hand, since the naturalness arguments are deep down statistical arguments, one might expect that an effective penalization of fine-tunings should arise from the Bayesian analysis itself, with no need of introducing "naturalness priors" or restricting the soft terms to the low-energy scale. It was shown in ref. [12] that this is indeed the case (see also [13] for a previous observation in this sense). The key point is the following. Normally, the value of μ (up to a sign) is deduced from the value of the other parameters by the condition that the Higgs vacuum expectation value is the correct one, or equivalently the $Z-$mass is the experimental one. However, this procedure does not incorporate the fact that such value of μ may involve an extreme fine-tuning, in which case should become statistically penalized. This shortcoming can be surmounted by simply considering $M_Z^{\rm exp}$ as experimental data on a similar foot to the others, entering the total likelihood, $\mathcal{L}$. For the sake of simplicity let us approximate the likelihood associated to the Z mass as a Dirac delta, so

$$p(\text{data}|s, m_0, m_{1/2}, A, B, \mu) \;\simeq\; \delta(M_Z - M_Z^{\rm exp})\; \mathcal{L}_{\rm rest}\;, \tag{2.4}$$

where $\mathcal{L}_{\rm rest}$ is the likelihood associated to all the physical observables, except M_Z. Now, we can take advantage of this Dirac delta to marginalize the posterior in one of the initial parameters, e.g. μ, performing a change of variable $\mu \to M_Z$:

$$\begin{aligned} p(s, m_0, m_{1/2}, A, B|\text{ data}) &= \int d\mu\; p(s, m_0, m_{1/2}, A, B, \mu|\text{data}) \\ &\simeq\; \mathcal{L}_{\rm rest} \left[\frac{d\mu}{dM_Z}\right]_{\mu_Z} p(s, m_0, m_{1/2}, A, B, \mu_Z)\;. \end{aligned} \tag{2.5}$$

where μ_Z is the value of μ that reproduces the experimental value of M_Z for the given values of $\{s, m_0, m_{1/2}, A, B\}$, and $p(s, m_0, m_{1/2}, A, B, \mu)$ is the prior in the initial parameters (still undefined). Note that the Jacobian factor, $\frac{d\mu}{dM_Z}$ can be written as $\frac{2\mu}{M_Z}\,\frac{1}{c_\mu}$, where $c_\mu = \left|\frac{\partial \ln M_Z^2}{\partial \ln \mu}\right|$ is the conventional Barbieri-Giudice measure [14, 15] of the degree of fine-tuning. Thus, the above Jacobian factor has built-in the desired fine-tuning penalization, with no ad hoc assumptions.

Actually this is enough to make the high-scale region of the parameter space, say soft terms $\gtrsim \mathcal{O}(10)$ TeV, statistically insignificant; which allows in turn to consider a wide range for the soft parameters (up to the very M_X). In consequence, the results of our analysis are essentially independent on the upper limits of the MSSM parameters, in contrast with previous studies.

Beside the above $\mu \to M_Z$ change of variable, it is highly advantageous for phenomenological studies to trade the Yukawa couplings by the physical fermion masses (which are easily marginalized out) and the initial $B-$parameter by the derived $\tan\beta = \langle H_u\rangle/\langle H_d\rangle$ parameter. Consequently we should compute the whole Jacobian, J, of the transformation

$$\{\mu, y_t, B\} \;\to\; \{M_Z, m_t, \tan\beta\}\ . \tag{2.6}$$

The initial prior (still undefined) is therefore always affected by this model-independent Jacobian factor, thus resulting in an *effective prior* in the new variables

$$p_{\rm eff}(g_i, m_t, m_0, m_{1/2}, A, \tan\beta) \;\equiv\; J|_{\mu=\mu_Z}\; p(g_i, y_t, m_0, m_{1/2}, A, B, \mu = \mu_Z)\ , \tag{2.7}$$

where we have already marginalized M_Z using the associated likelihood $\sim \delta(M_Z - M_Z^{\rm exp})$ (recall that μ_Z is the value of μ that reproduces the experimental M_Z.) In eqs.(2.6, 2.7) we have made explicit the dependence just on the top Yukawa coupling and mass, but for other fermions goes the same.

So, to prepare the scan in the new variables we need an explicit evaluation of the Jacobian factor. For the numerical analysis we have evaluated J using the `SoftSusy` code [16] which implements the full one-loop contributions and leading two-loop terms to the tadpoles for the electroweak breaking conditions with parameters running at two-loops. This essentially corresponds to the next-to-leading log approximation; see ref. [17, 18, 19, 20] for details.

However, it is possible to give an analytical and quite accurate expression of J, and thus of the effective prior, by working with the tree-level potential with parameters running at one-loop (i.e. essentially the leading log approximation). At this level, the relation of $\{\mu, y_t, B\}$ with $\{M_Z, m_t, \tan\beta\}$ is given by the minimization conditions and the expression for the (running) top mass,

$$\mu^2_{\rm low} = \frac{m^2_{H_d} - \tan^2\beta\; m^2_{H_u}}{\tan^2\beta - 1} - \frac{M_Z^2}{2} \tag{2.8}$$

$$B_{\rm low} = \frac{s_{2\beta}}{2\mu_{\rm low}}(m^2_{H_1} + m^2_{H_2} + 2\mu^2_{\rm low}) \tag{2.9}$$

$$y_{\rm low} = \frac{m_t}{v\ s_\beta}\ . \tag{2.10}$$

Here y denotes the top Yukawa coupling and the "low" subscript indicates that the quantity is evaluated at low scale (more precisely, at a representative supersymmetric mass, such as the geometric average of the stop masses). The soft masses $m^2_{H_u}, m^2_{H_d}$ are also understood at low scale. For notational simplicity, we have dropped the subscript t from the Yukawa coupling. (Note that all these low-energy quantities contain an implicit dependence on the top Yukawa coupling through the corresponding RG equations.) Then

$$J \propto \left[\frac{E}{R_\mu^2}\right]\ \frac{y}{y_{\rm low}}\frac{\tan^2\beta - 1}{\tan\beta(1+\tan^2\beta)}, \tag{2.11}$$

where R_μ and E are defined through the renormalization group equations of μ and y,

$$\mu_{\rm low} = R_\mu(y)\mu, \quad y_{\rm low} \simeq \frac{yE(Q_{\rm low})}{1+6yF(Q_{\rm low})}\ . \tag{2.12}$$

Here Q is the renormalization scale, $F = \int_{Q_{\rm high}}^{Q_{\rm low}} E \ln Q$, and $E(Q)$ is a definite function that depends just on the gauge couplings [21][1].

The important point is that the Jacobian (2.11) is a model-independent factor, valid for any MSSM, which must be multiplied by whatever prior is chosen for the initial parameters. It *cannot* be ignored. Hence, the effective prior in the standard variables $\{m_t, m_0, m_{1/2}, A, \tan\beta\}$ reads

$$p_{\rm eff}(m_t, m_0, m_{1/2}, A, \tan\beta)\ \propto\ \left[\frac{E}{R_\mu^2}\right]\ \frac{y}{y_{\rm low}}\frac{\tan^2\beta - 1}{t(1+\tan^2\beta)}\frac{B_{\rm low}}{\mu_Z}\ p(m_0, m_{1/2}, A, B, \mu_Z), \tag{2.13}$$

where all the subjectivity lies in the $p(m_0, m_{1/2}, A, B, \mu)$ piece, i.e. the prior in the initial parameters, for which we have still to make a choice (we will do it in the next subsection). This Jacobian (model-independent) prefactor contains the above-discussed penalization of fine-tuned regions. Thus, using it automatically incorporates the fine-tuning penalizations with no ad hoc assumptions. Note that, besides the penalization for large μ, the Jacobian factor contains a penalization of large $\tan\beta$, reflecting the smaller statistical weight of this possibility. Actually, the implicit fine-tuning associated to a large $\tan\beta$ was already noted in ref. [22, 23], where it was estimated to be of order $1/\tan\beta$, in agreement with eq.(2.13).

2.3 Priors in the initial parameters

The choice of the prior in the initial parameters, $\{m_0, m_{1/2}, A, B, \mu\}$ must reflect our knowledge about them, before consideration of the experimental data (to be included in the likelihood piece). Four of them, $\{m, M, A, B\}$, are soft SUSY-breaking parameters. They typically go like $\sim F/\Lambda$, where F is the SUSY breaking scale, which corresponds to the dominant VEV among the auxiliary fields in the SUSY breaking sector (it can be an $F-$term

[1] Besides an (irrelevant) numerical factor, the expression (2.11) contains a $\sin\beta$ factor which is cancelled assuming, as usual, a logarithmically flat prior for the Yukawa coupling, i.e. $p(y) \propto y^{-1}$.

or a $D-$term) and Λ is the messenger scale, associated to the interactions that transmit the breaking to the observable sector. Since the soft-breaking terms share a common origin it is logical to assume that their sizes are also similar. Of course, there are several contributions to a particular soft term, which depend on the details of the superpotential, the Kähler potential and the gauge kinetic function of the complete theory (see e.g. ref. [24]). So, it is reasonable to assume that a particular soft term can get any value (with essentially flat probability) of the order of the typical size of the soft terms or below it. The $\mu-$parameter is not a soft term, but a parameter of the superpotential. However, it is desirable that its size is related (e.g. through the Giudice-Masiero mechanism [25]) to the SUSY breaking scale. Otherwise, one has to face the so-called $\mu-$problem, i.e. why should be the size of μ similar to the soft terms', as is required for a correct electroweak breaking [see eq.(2.8)]. Thus, concerning the prior, we can consider μ on a similar foot to the other soft terms.

Let us denote M_S the typical size of the soft terms in the observable sector, $M_S \sim F/\Lambda$. Then, we define the ranges of variation of the initial parameters as

$$\begin{aligned} -qM_S \leq \quad & B \quad \leq qM_S \\ -qM_S \leq \quad & A \quad \leq qM_S \\ 0 \leq \quad & m_0 \quad \leq qM_S \\ 0 \leq \; & m_{1/2} \leq qM_S \\ 0 \leq \quad & \mu \quad \leq qM_S \end{aligned} \tag{2.14}$$

where q is an $\mathcal{O}(1)$ factor. We have considered here the branch of positive μ. For the negative one we simply replace $\mu \to -\mu$. We can take $q = 1$ with no loss of generality, provided M_S is allowed to vary in the range $0 \leq M_S \leq \infty$. In practice, to avoid divergences in the priors, we have to take a finite range for M_S, say

$$M_S^0 \leq M_S \leq M_X \,, \quad M_S^0 \sim 10 \text{ GeV} \tag{2.15}$$

Nevertheless, the values of the upper and lower limits of the M_S range are *irrelevant*. A small value for M_S (as the above lower limit) is in practice excluded by the LHC exclusion limits. A high value for M_S (as the above upper limit) is in practice statistically irrelevant thanks to the Jacobian prefactor in eq.(2.7) or eq.(2.13), i.e. by the naturalness of the EW breaking. So the results of the present approach are certainly independent of the ranges established for the parameters, something very satisfactory.

Concerning the shape of the priors, as already stated, we find reasonable to assume (conveniently normalized) flat priors for the soft parameters inside the ranges (2.14), i.e.

$$p(m_0) = p(m_{1/2}) = p(\mu) = \frac{1}{M_S} \,, \quad p(A) = p(B) = \frac{1}{2M_S}. \tag{2.16}$$

The next step is to choose a prior for M_S. Admittedly, this is the less objective part of the statistical analysis, but, as discussed above, one cannot simply ignore the prior; it is an unavoidable piece when one wants to determine the probability distribution in the parameter space. The most conservative attitude is to use two different, though still

reasonable, priors, and then compare the results. This gives a fair measure of the prior-dependence.

For that matter we have considered two somehow standard types of prior: flat and logarithmic. In a flat (logarithmic) prior one assumes that, in principle, the typical size (order of magnitude) of the soft terms can be anything, say from M_S^0 up to M_X, with equal probability. In our opinion, a logarithmic prior is probably the most reasonable option, since it amounts to consider all the possible magnitudes of the SUSY breaking in the observable sector on the same foot (this occurs e.g. in conventional SUSY breaking by gaugino condensation in a hidden sector). However, we will consider log and flat priors at the same level throughout the paper, in order to compare the results and thus evaluate the prior-dependence.

Finally, we can marginalize M_S, which thus disappears completely from the subsequent analysis, leaving a prior which depends just on the $\{m_0, m_{1/2}, A, B, \mu\}$ parameters[2]. Using eqs.(2.16), one gets, for the logarithmic case,

$$\begin{aligned} p(m_0, m_{1/2}, A, B, \mu) &\propto \int_{\max\{m_0, m_{1/2}, |A|, |B|, \mu, M_S^0\}}^{M_X} \frac{1}{M_S^6}\, dM_S \\ &\simeq \frac{1}{[\max\{m_0, m_{1/2}, |A|, |B|, \mu, M_S^0\}]^5} \end{aligned} \tag{2.17}$$

which is the prior to be plugged in eq.(2.7) (or in the approximated expression (2.13)) to get the effective prior in the scan parameters. For the flat case, the analogous computation gives

$$p(m_0, m_{1/2}, A, B, \mu) \propto \frac{1}{[\max\{m_0, m_{1/2}, |A|, |B|, \mu, M_S^0\}]^4}. \tag{2.18}$$

The fact that eqs.(2.17, 2.18) correspond, respectively, to logarithmic and flat priors in the size of the soft terms can be verified by marginalizing all the soft parameters but one, say $m_{1/2}$, before incorporating any experimental information. Then one does obtain logarithmic and flat behaviors, respectively, as is clear from the exponents in the above denominators (for a more throughout discussion see ref. [27]).

3. Physical observables and computational methods used in the analysis

A first group of physical observables used in the analysis are the SM-like parameters, e.g. masses and couplings of SM particles. Some of them, in particular the top and bottom masses and the electromagnetic and strong coupling constants, have a strong influence in the analysis. We have treated them as nuisance variables (marginalizing them) using the central values and uncertainties given in Table 1

Furthermore, the full set of experimental data used to compute the likelihood function is listed in Table 2. The full likelihood function is the product of the individual likelihoods

[2]This procedure is a "hierarchical Bayesian technique", first used in ref. [26], but using complicated functions that were not possible to integrate analytically.

SM nuisance parameters			
	Gaussian prior	Range scanned	ref.
M_t [GeV]	173.2 ± 0.9	(167.0, 178.2)	[28]
$m_b(m_b)^{\bar{M}S}$ [GeV]	4.20 ± 0.07	(3.92, 4.48)	[29]
$[\alpha_{em}(M_Z)^{\bar{M}S}]^{-1}$	127.955 ± 0.030	(127.835, 128.075)	[29]
$\alpha_s(M_Z)^{\bar{M}S}$	0.1176 ± 0.0020	(0.1096, 0.1256)	[30]

Table 1: Nuisance parameters adopted in the scan of the CMSSM parameter space, indicating the mean and standard deviation adopted for the Gaussian prior on each of them, as well as the range covered in the scan.

associated to each piece of experimental data. As discussed in the next section, not all those observables are included in the computation of the full likelihood all the time. In particular, we plug and unplug the dark matter constraints to check its impact. For the quantities for which positive measurements have been made (as listed in the upper part of Table 2), we assume a Gaussian likelihood function with a variance given by the sum of the theoretical and experimental variances, as motivated by eq. (3.3) in ref. [31]. For the observables for which only lower or upper limits are available (as listed in the bottom part of Table 2) we use a smoothed-out version of the likelihood function that accounts for the theoretical error in the computation of the observable, see eq. (3.5) and fig. 1 in ref. [31].

Let us comment briefly on some of the observables and the theoretical method used to compute the theoretical prediction for them and the corresponding likelihood.

To calculate the MSSM spectrum we have used `SoftSusy` [16], where SUSY masses are computed at full one-loop level and the Higgs sector includes two-loop leading corrections [44]. We discard points suffering from unphysicalities: no self-consistent solutions to the RGEs, no EW breaking and tachyonic states. In our treatment of the radiative corrections to the electroweak observables M_W and $\sin^2\theta_{\rm eff}$ we include full two-loop and known higher order SM corrections as computed in ref. [45, 46], as well as gluonic two-loop MSSM corrections obtained in [47].

The most important piece of experimental information is by far the Higgs mass, m_h, for which we use the value obtained from the combination of the ATLAS and CMS experimental results, expressed in eq.(1.2). At each point of the supersymmetric parameter-space we evaluate the theoretical prediction for m_h through `SoftSusy`, which has the two-loop computation incorporated. The estimated theoretical uncertainty is ± 2 GeV.

Concerning B-physics, the branching ratio for the $B \to X_s\gamma$ decay (the most important one) has been computed with the numerical code `SusyBSG` [48] using the full NLO QCD contributions, including the two-loop calculation of the gluino contributions presented in [49] and the results of [50] for the remaining non-QCD $\tan\beta$-enhanced contributions. The supersymmetric contributions to $b \to s\gamma$ grow with decreasing masses of the supersymmetric particles *and* with increasing $\tan\beta$. The other B(D)-physics observables summarized in Table 2 have been computed with the code `SuperIso` (for details on the computation of

Observable	Mean value	Uncertainties		ref.
	μ	σ (exper.)	τ (theor.)	
M_W [GeV]	80.399	0.023	0.015	[32]
$\sin^2\theta_{eff}$	0.23153	0.00016	0.00015	[32]
$BR(\overline{B} \to X_s\gamma) \times 10^4$	3.55	0.26	0.30	[33]
$R_{\Delta M_{B_s}}$	1.04	0.11	-	[34]
$\frac{BR(B_u\to\tau\nu)}{BR(B_u\to\tau\nu)_{SM}}$	1.63	0.54	-	[33]
$\Delta_{0-} \times 10^2$	3.1	2.3	-	[35]
$\frac{BR(B\to D\tau\nu)}{BR(B\to De\nu)} \times 10^2$	41.6	12.8	3.5	[36]
R_{l23}	0.999	0.007	-	[37]
$BR(D_s \to \tau\nu) \times 10^2$	5.38	0.32	0.2	[33]
$BR(D_s \to \mu\nu) \times 10^3$	5.81	0.43	0.2	[33]
$BR(D \to \mu\nu) \times 10^4$	3.82	0.33	0.2	[33]
$BR(\overline{B}_s \to \mu^+\mu^-)$	3.2×10^{-9}	1.5×10^{-9}	10%	[38]
$\Omega_\chi h^2$	0.1109	0.0056	0.012	[39]
m_h [GeV]	125.85	0.4	2	[40]
	Limit (95% CL)		τ (theor.)	ref.
Sparticle masses	As in table 4 of ref. [31].			
$m_0, m_{1/2}$	LHC exclusion limits, see text			[41]
$m_A, tan\beta$	LHC exclusion limits, see text			[42]
$m_\chi - \sigma^{\rm SI}_{\chi-p}$	XENON100 2012 limits (224.6 × 34 Kg days)			[43]

Table 2: Summary of the observables used for the computation of the likelihood function For each quantity we use a likelihood function with mean μ and standard deviation $s = \sqrt{\sigma^2 + \tau^2}$, where σ is the experimental uncertainty and τ represents our estimate of the theoretical uncertainty. Lower part: Observables for which only limits currently exist. The explicit form of the likelihood function is given in ref. [31], including in particular a smearing out of experimental errors and limits to include an appropriate theoretical uncertainty in the observables.

the observables see [51] and references therein). Among them is the $BR(\overline{B}_s \to \mu^+\mu^-)$ for which we include the new LHCb measurement $(3.2^{+1.5}_{-1.2}) \times 10^{-9}$, derived from a combined analysis of 1 fb^{-1} data at $\sqrt{s} = 7$ TeV collision energy and 1.1 fb^{-1} data at $\sqrt{s} = 8$ TeV collision energy [38]. We implement this constraint as a Gaussian distribution with a conservative experimental error of $\sigma = 1.5 \times 10^{-9}$, and a 10% theoretical error. Both codes have been integrated into the forthcoming `SuperBayes-v2.0` code [52].

We also include recent data from the XENON100 direct detection experiment, obtained with an effective volume of 34 kg and an exposure of 224.6 days between February 2011 and March 2012 [43]. Two candidate scattering events were detected within the signal region, with an expected number background of $b = 1.0 \pm 0.2$ events, resulting in exclusion limits in the $(m_{\tilde{\chi}^0_1}, \sigma^{\rm SI}_{\chi-p})$ plane. The corresponding likelihood function is described in detail in ref. [11], which we refer the reader to for further details.

In addition, we incorporate the most recent constraints from SUSY searches at the LHC. We follow the analysis presented by the ATLAS collaboration in ref. [53], since it

is the one associated to the more stringent constraints: a data sample corresponding to a luminosity of 5.8 fb^{-1} for a center-of-mass energy of $\sqrt{s} = 8$ TeV in the 0-lepton channel. As no significant deviations have been so far found with respect to SM predictions, this has been used to derive the constraints on the $(m_0, m_{1/2})$ plane [41]. We note that while this 95% exclusion line has been obtained assuming values of $\tan\beta = 10$ and $A_0 = 0$ GeV, the final result is not expected to change much for different values of these two parameters since the production and decay of squarks and gluinos are quite insensitive to the values of $\tan\beta$ and A_0 [54] . Besides, we have applied this limit to the NUHM since the SUSY signal for gluino and squarks production does not depend significantly on other parameters than m_0 and $m_{1/2}$. Additionally we have included exclusion limit in the (m_A,$\tan\beta$) plane from a CMS search for the decay of neutral Higgs bosons into final states containing two muons and missing E_T, based on 4.5 fb^{-1} integrated luminosity of data collected at $\sqrt{s} = 7$ TeV collision energy [42]. We include those exclusion limits by assigning a likelihood equal to zero to samples falling below the exclusion line.

As a scanning algorithm we adopt the MultiNest [55] algorithm as implemented in `SuperBayeS-v2.0`. It is based on the framework of Nested Sampling, invented by Skilling [56, 57]. MultiNest has been developed in such a way as to be an extremely efficient sampler even for likelihood functions defined over a parameter space of large dimensionality with a very complex structure as it is the case of the CMSSM. The main purpose of the Multinest is the computation of the Bayesian evidence and its uncertainty but it produces posterior inferences as a by–product. For the marginalization procedure we have used the above-discussed ranges for our priors. Besides, we have considered $2 < \tan\beta < 62$, although the precise limits of this range are irrelevant. A too low value of $\tan\beta$ is excluded by the Higgs mass value, unless the supersymmetric masses are extremely high, which is drastically disfavoured by the naturalness of the EW breaking through the above-discussed Jacobian factor. (More precisely, $\tan\beta = 2$ requires stop masses above 10^3 TeV [58, 59]). On the other hand, the region of very large $\tan\beta$ is also strongly suppressed by the EW mechanism, as is clear by the prefactor in eq.(2.13).

4. Results for the CMSSM

We have organized the presentation of the results in following way.

In subsect. 4.1 we show the plots of the probability distribution function (in one and two dimensions) using only the most robust group of experimental data, namely LHC exclusion limits, Higgs mass, and EW- and B(D)-physics observables. At this stage we leave aside dark matter constraints since supersymmetric dark matter could be unestable with a tiny amount of R-parity violation (without modifying the rest of the analysis). In that case the dark matter constraints would be irrelevant. In subsect. 4.2 we include the dark matter constraints in two different fashions: either requiring that the supersymmetric dark matter is consistent with actual dark matter observed abundance or less than it. Note that the latter, more conservative, case could be realistic if there is an additional source of dark matter (such as axions). In subsect. 4.3 we discuss the g-2 issue. Along this section

we present the results just for the CMSSM scenario. The results for the NUHM one are presented in section 6 following a similar scheme.

4.1 Results with no dark matter constraints

At this stage we have used all the observables, except those related to dark matter.

In fig. 1 we present the probability distribution function (posterior) for the four CMSSM parameters, $m_0, m_{1/2}, A, \tan\beta$, and the physical gluino and (first and second generation) squark masses. For each case, the non-plotted parameters have been marginalized. The red(cyan) lines show the results for flat(logarithmic) priors All the plots in fig. 1 correspond to positive μ. The results for negative μ are almost identical, so we do not show them to avoid proliferation of figures.

Fig. 2 shows the probability distribution functions for flat and log priors when all parameters except two are marginalized. This gives rise to the two-dimensional plots in the $m_0 - m_{1/2}$ and $m_{\tilde{q}} - m_{\tilde{g}}$ planes. The present LHC limits (at 5.8 fb^{-1})[41] and the expected ones in the future (3000 fb^{-1})[60] are shown for reference.

Clearly, the bulk of the probability lies in the high-energy region which is not directly accessible to the LHC at present. The rather high Higgs mass reported by ATLAS and CMS is the main responsible of this effect. As it is well-known, in the MSSM the tree-level Higgs-mass in the MSSM is bounded by the mass of the Z-boson, so large radiative corrections are needed in order to reconcile theory and experiment. An approximate analytic formula for m_h [61, 62, 63, 64, 65, 66, 20, 67], useful for discussions, reads

$$m_h^2 \simeq M_Z^2 \cos^2 2\beta + \frac{3}{4\pi^2}\frac{m_t^4}{v^2}\left[\log\frac{M_{\rm SUSY}^2}{m_t^2} + \frac{X_t^2}{M_{\rm SUSY}^2}\left(1 - \frac{X_t^2}{12 M_{\rm SUSY}^2}\right)\right] + \cdots \qquad (4.1)$$

where m_t is the top running mass, $M_{\rm SUSY}$ represents a certain average of the stop masses and $X_t = A_t - \mu\cot\beta$ [65, 20, 67]. The first term of (4.1) is the tree-level Higgs-mass and the second are the dominant radiative and threshold contributions. Note that the radiative corrections grow logarithmically with the stop masses while the threshold correction has a maximum for $X_t = \pm\sqrt{6}M_{\rm SUSY}$.

The important point is that, in order to achieve $m_h = 125 - 126$ GeV, one typically needs (besides non-small $\tan\beta$) stop masses $\gtrsim 3$ TeV, unless X_t happens to be close to the above-mentioned maximizing value (we will comment on the latter possibility below). This is what the probability distributions of Figs. 1, 2 show. It should be kept in mind that in the CMSSM all squark masses come from a universal value at M_X, so it is not possible to have large stop masses (required to reproduce the value of m_h) and lighter masses for the other squarks. In a general MSSM Figs. 1, 2 would approximately represent the constraints on the third-generation squark masses and trilinear coupling, and on the gluino mass (at M_X and at low-energy).

Of course, these kinds of results are known and expected; but the present Bayesian analysis allows to quantify the effect, showing the new probability distribution functions of the various parameters.

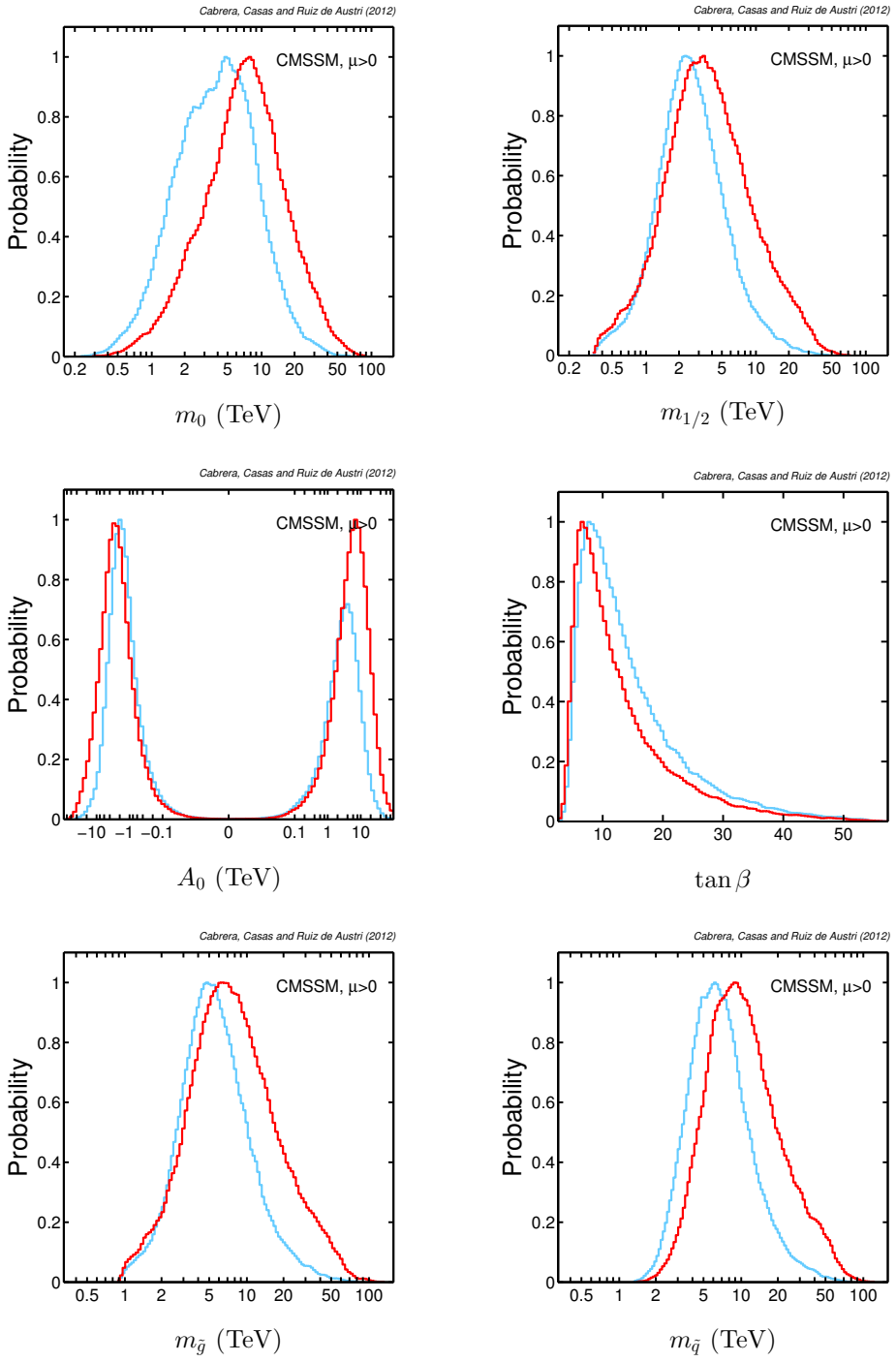

Figure 1: 1D marginalized posterior probability distribution of the CMSSM parameters: $m_0, m_{1/2}, A, \tan\beta$ and the physical squark (of the first two generations) and gluino masses. The red(cyan) corresponds to flat(logarithmic) priors.

The results of Figs. 1, 2 show clearly that, with the present information, the probability of detecting the CMSSM at present at the LHC (even if it is the true model) are $\lesssim 5\%$,

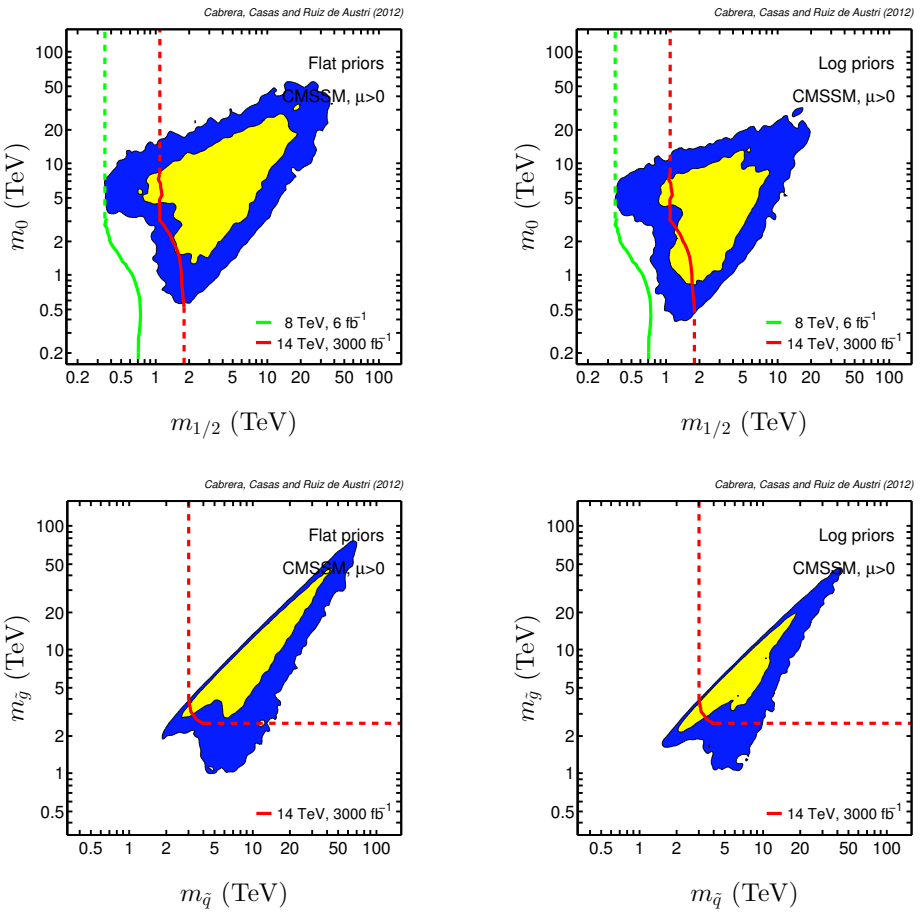

Figure 2: 2D marginalized posterior probability distribution of the CMSSM in the $m_{1/2} - m_0$ and the $m_{\tilde{g}} - m_{\tilde{q}}$ planes. Left panels show the flat priors case and right panels the logarithmic one. Both for $\mu > 0$. The inner and outer contours enclose respective 68% and 95% joint regions.

at least with the current techniques to search for physics beyond the SM in LHC data. In the long-term future the probability is substantially higher, but still the chances of *not* discovering it are larger. To put this in optimistic/wishful-thinking terms, since $m_h \simeq 126$ GeV, if one believes in the CMSSM one should not be worried about the no-detection of SUSY at LHC up to now! But its detection in the future will be challenging too. This is the main conclusion of the Bayesian analysis at this stage.

On the other hand, it should be kept in mind that in a Bayesian analysis one assumes that the scenario studied (in this case the CMSSM) is the true one, and then one determines the probability distribution in the parameter space. It does not give a direct measure of how likely is the scenario itself, unless one compares it with an alternative scenario using evidence-comparison techniques. We will come back to this point in the discussion of sect. 6 below. But it is already clear that the experimental results on the Higgs mass have pushed the probability to a region which was statistically disfavored (fine-tuned) before the discovery, which sheds shadows on the naturalness of the CMSSM. In sect. 6 we will

make this point more quantitative.

Let us comment now on other interesting aspects of the results shown in Figs. 1, 2. As already mentioned, the results for negative μ are almost the same. The experimental Higgs mass requires heavy supersymmetric particles, which makes SUSY decoupled for many purposes and makes all the sign μ effects in observables (e.g. electroweak and $B-$physics observables) rather irrelevant. An exception to this would be the $g-2$ data, which have not been included in the analysis for the reasons explained in subject. 4.3. On the other hand it is quite remarkable the stability of the results against changes in the priors. Although the log priors prefer logically slightly lower values of the supersymmetric masses, the difference is not significant. This is quite satisfactory, showing that the experimental data are already able to determine pretty unambiguously the preferred supersymmetric regions in the parameter space. Still, how ever, the acceptable ranges for the supersymmetric parameters are quite wide, but systematically beyond 1 TeV.

The probability distribution for $\tan\beta$, with a maximum around $\tan\beta \sim 6$, is originated by two opposed effects. On the one hand, the large experimental Higgs mass favors large $\tan\beta$, since the tree-level contribution to m_h is proportional to $\cos^2 2\beta$ and therefore grows with $\tan\beta$; although the effect is negligible beyond $\tan\beta \simeq 8$. On the other hand the Jacobian factor (2.11) penalizes large $\tan\beta$, due to the implicit fine-tuning among the initial parameters required to obtain it.

The A_0 parameter shows two wide peaks for positive and negative values, see fig. 1. This effect is in fact due to the logarithmic scale used for the representation. In a linear scale, the probability presents just one peak in the central region. On the other hand, it can be noticed that the preferred positive values of A_0 tend to be larger than the negative ones. This comes from the fact that the RG equations drive A towards negative values, which increases (decreases) its absolute value if its initial sign is negative (positive). Thus a too large initial negative value of A_0 gives too large values of A at low energy, leading to the appearance of tachyons.

The discussion of the $A-$parameter raises another important point. As mentioned above, the value of m_h is maximized for $X_t = \pm\sqrt{6}M_{\rm SUSY}$. In that case, lower masses for the stops are acceptable, which in principle would make SUSY less fine-tuned. This possibility is certainly interesting. However, it represents itself another kind of fine-tuning unless one has some theoretical reason to expect X_t in the favorable range. Incidentally, note that for moderately large $\tan\beta$ the value of X_t is essentially given by A_t, so one would essentially need a value of A_t in the favorable range. In any case, this would amount to go beyond the MSSM, e.g. invoking a particular SUSY breaking and mediation mechanism that could lead to this result for A_t [3]. If we do not rely on a mechanism of that kind, the question is whether it pays or not (in statistical weight) to have X_t around the maximal value. This question is answered by the Bayesian analysis. If the answer is positive, the value of X_t should be concentrated around that privileged value. Fig. 3 shows the probability distribution function in the plane $m_h - (X_t/M_S)$ (all the remaining parameters

[3] See ref.[68] for a paper arguing that this can actually occur in a class of superstring scenarios.

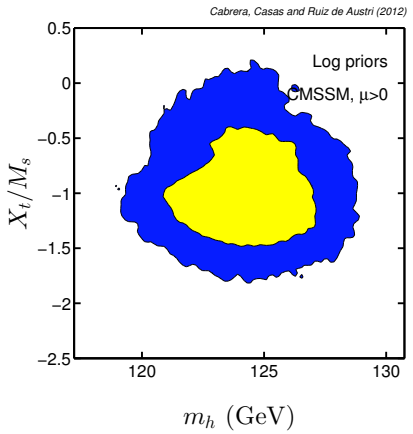

Figure 3: 2D marginalized posterior probability distribution of the CMSSM in the m_h–X_t/M_S plane, using log priors for $\mu > 0$. The inner and outer contours enclose respective 68% and 95% joint regions.

are marginalized). Clearly, the probably does not show any preference for that value. In other words, requiring that value for X_t implies a more severe fine-tuning than living with rather large squark masses.

4.2 Incorporation of dark matter

There are different astrophysical and cosmological observations that offer impressive evidence of the existence of dark matter (DM) in the Universe (see Table 2 for a recent determination of $\Omega_{\rm DM}$). On the other hand, the consistency with the observed large structure of the Universe favours cold dark matter (CDM), i.e. non-relativistic matter at the beginning of galaxy formation. This leads to the hypothesis of a weakly interacting massive particle (WIMP) as the component of CDM.

Supersymmetry offers a good candidate for such a WIMP, namely the LSP, which is stable in the standard (R-parity conserving) SUSY formulations (for a review see [69]). Although, depending on the models, there are several possibilities for the SUSY WIMP, the most popular and natural candidate is the lightest neutralino (from here on we will refer it as the neutralino), χ_1^0, which is the LSP in most of the CMSSM parameter space. One could assume that the LSP makes up the whole content of DM required by the "standard" cosmology. However, it could happen that the early thermal production of WIMPs is diluted by electroweak inflation. Admittedly, the latter is not a most natural or popular scenario of inflation, but mechanisms for it have been explored [70]. Alternatively, the LSP could be unstable assuming tiny violations of R-parity, see e.g. [71]. In these cases the observed dark matter should be provided by other candidate, e.g. an axion.

Motivated for this, we discuss next, separately, the cases where the DM is made only of LSPs and where it is partially made of LSPs.

Single-Component DM

In this scenario we assume a Gaussian likelihood on $\Omega_\chi h^2$ (see Table 2). Besides, we apply the constraints from DM-induced recoil events in the XENON100 experiment, as described above. For the present analysis we neglect the effect of the astrophysical and hadronic uncertainties entering into the determination of the spectrum of recoil events. Namely, we fix the astrophysical parameters that describe the density and velocity distribution of DM particles at the commonly adopted benchmark values: local CDM density $\rho_{\odot,\mathrm{CDM}} = 0.4\,\mathrm{GeV\,cm^{-3}}$, circular velocity $v_0 = 235$ km s^{-1} and escape velocity $v_{esc} = 550$ km s^{-1} (see, e.g., [72] and references therein for a recent discussion of the astrophysical uncertainties on these quantities). For the contribution of the light quarks to the nucleon form factors we have adopted the values $f_{Tu} = 0.02698$, $f_{Td} = 0.03906$ and $f_{Ts} = 0.36$ [73]. Incorporating the associated uncertainties of both the astrophysical and nuclear form factors parameters to the analysis as nuisance parameters (i.e. marginalizing) would only mildly change the numerical results presented here; the main conclusions would remain unchanged, in agreement with the findings of [74].

In fig. 4 we plot the 1D pdfs of various supersymmetric parameters and the physical gluino and squark masses. The cyan-continuous (blue-dashed) line corresponds to $\mu > 0$ ($\mu < 0$). This is complemented with the 2D pdfs of fig. 5. In all cases the non-displayed parameters have been marginalized. The results correspond to log priors (for flat priors they are very similar). The first thing to notice is that, due to the DM constraints, the pdfs of $m_{1/2}$ and m_0 (an thus of $m_{\tilde{g}}, m_{\tilde{q}}$) have moved further to large values. Indeed, more than the 95% of the posterior probability is out of the LHC reach, even with an energy of 14 TeV and a integrated luminosity of 3000 fb^{-1} as projected for the HL-LHC (High Luminosity) phase. [60]. This conclusion holds for the flat priors case. The reason is the following. There are in fact two additional regions where the required DM abundance can be reproduced: the stau-coannihilation and the $A-$funnel regions. However, the first one is disfavored, as it corresponds to rather small soft terms, difficult to reconcile with the Higgs mass. The second one requires intermediate/large $\tan\beta$ values, which are penalized by the Jacobian prefactor in the r.h.s. of eq.(2.13). In consequence, one is essentially left with the Focus-Point region (actually the other two regions survive but with very tiny statistical weight, as discussed in sect. 7).

In Appendix A we describe some characteristics of the Focus-Point in the CMSSM and the NUHM. Let us now mention some of them, which will be useful to understand the shape of Figs. 4, 5. The Focus-Point region corresponds to heavy scalars (m_0), less heavy gauginos ($m_{1/2}$) and $\tan\beta \gtrsim 8$. In that region the value of $m^2_{H_u}$ at low energy is quite insensitive to its value at high-energy, this is the reason why it can reach large values with no additional fine-tuning. For too-large m_0, however, the electroweak breaking solution gets lost. This occurs when the required value of μ^2 gets negative. For slightly smaller values of m_0 the value of μ is small, and this is welcome for fine-tuning reasons, since the Jacobian prefactor in eq.(2.13) gets smaller. Hence, this is a theoretically interesting region by itself. But, besides, it is also appropriate to correctly reproduce the DM abundance. The reason is that

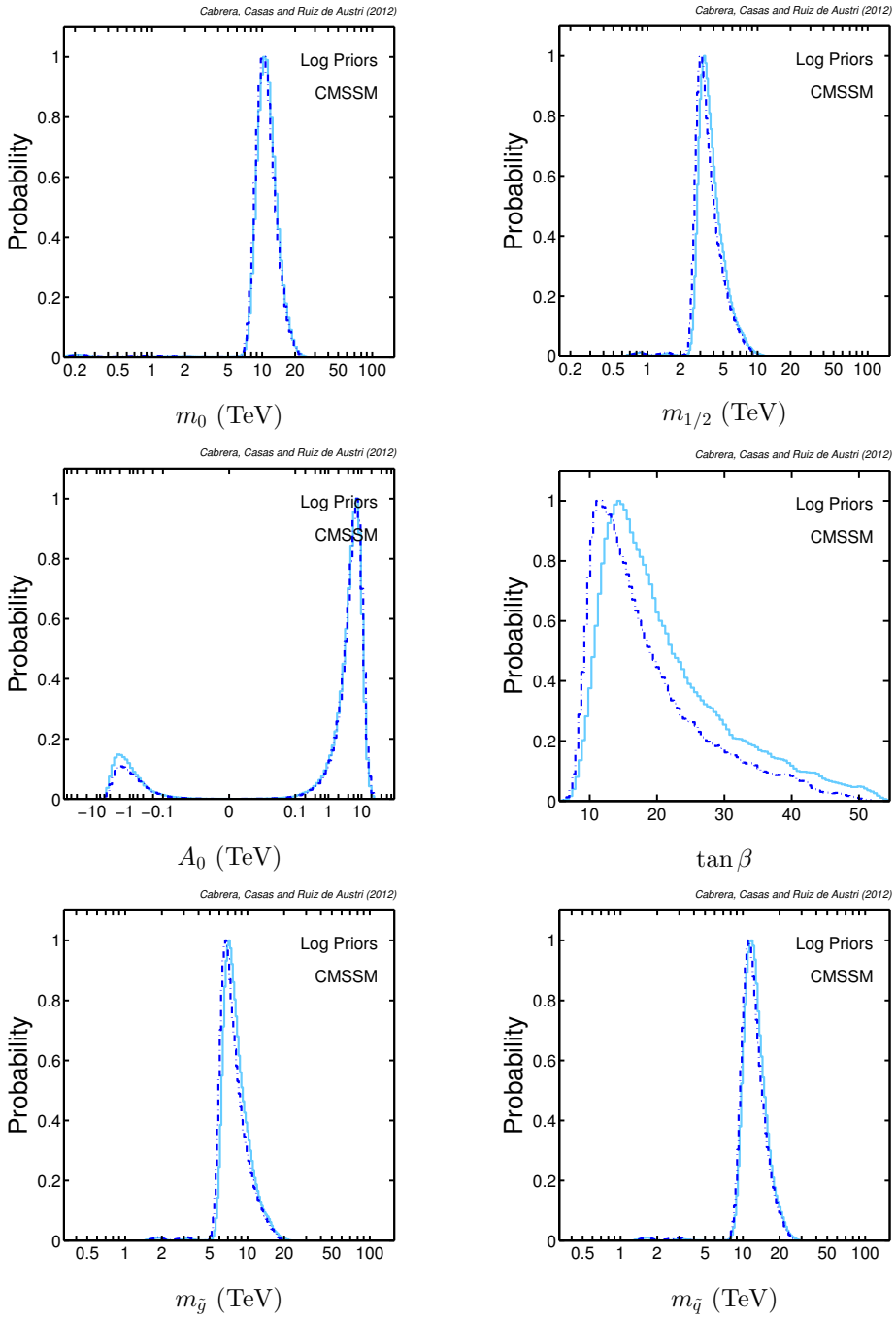

Figure 4: As in fig. 1 but with an additional constraint from DM (WMAP 7-years and XENON100) considering that the lightest supersymmetric particle (LSP) is the soley DM component. Here the cyan line corresponds to a positive μ whereas the blue dashed to a negative μ.

if μ is smaller than (or similar to) $m_{1/2}$, the light est neutralino is essentially a Higgsino (or a mixture of Higgsino and bino). That sizable fraction of Higgsino makes the neutralinos to coannihilate efficiently with the lightest chargino and the second lightest neutralino, which

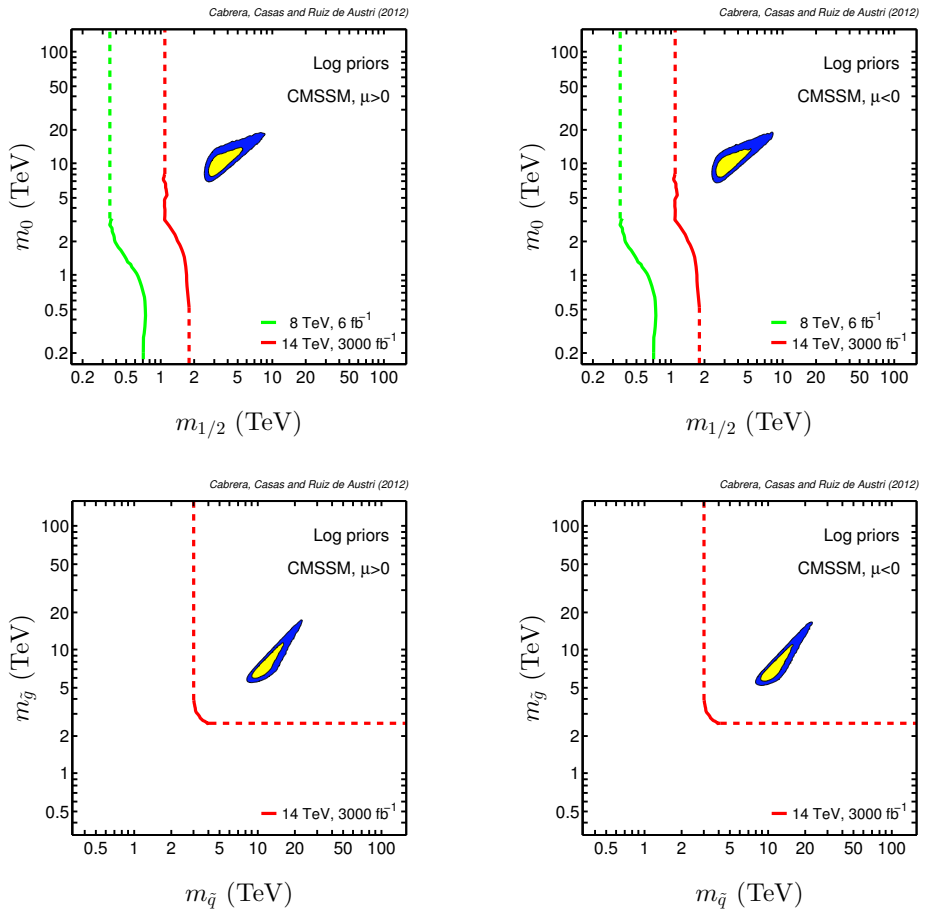

Figure 5: As in fig. 2 but with an additional constraint from DM (WMAP 7-years and XENON100) considering that the LSP is the soley DM component.

may lead to the correct DM abundance. Actually, if the lightest neutralino is essentially a pure Higgsino and its mass is too small, the annihilation is too efficient. Then one needs a sizable bino component to reduce the annihilation so that the correct DM abundance is reproduced. Therefore the largest acceptable neutralino mass corresponds to the pure Higgsino case, and is $M_\chi \simeq 1$ TeV [75] (in that limiting case the neutralino, chargino, and second neutralino masses are all $\sim \mu$). Below that limit, the neutralino mass can vary in a wide range, provided it contains the suitable bino fraction. Indeed, this was the situation prior to the new XENON100 data.

The point is that XENON is sensitive to the spin-independent cross-section of $O(100)$ GeV neutralinos with the nucleons, if the former contain both a Higgsino and bino components. This occurs through diagrams exchanging a Higgs state. In this way XENON100 has been able to exclude all the above-mentioned Focus-Point region, whenever there is a non-negligible Higgsino-bino mixture. In essence, only the pure Higgsino possibility remains alive [5]. In consequence the value of m_χ and μ are constrained around 1 TeV. In addition, the bino mass cannot be smaller than that, otherwise the lightest neutralino

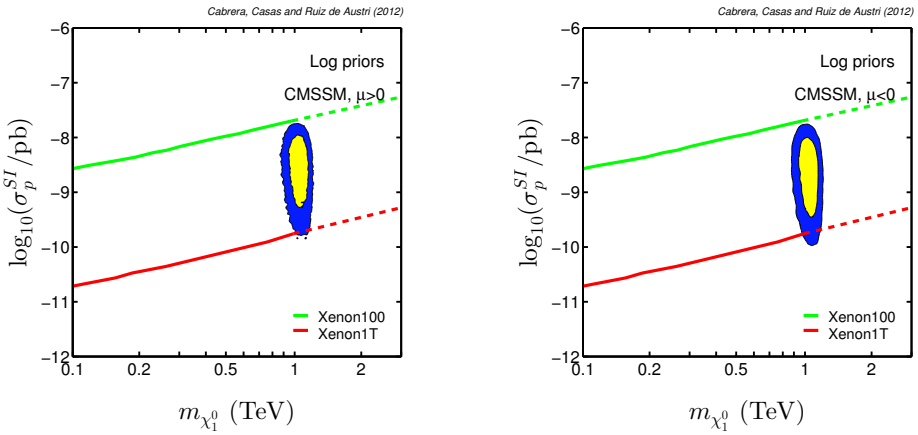

Figure 6: 2D marginalized posterior probability distribution of the spin–independent scattering cross section of a neutralino off a proton versus neutralino mass being this the soley DM component for log priors, $\mu > 0$ (left panel) and $\mu < 0$ (right panel).

.

would get a sizable bino component, which is excluded by XENON. This is the reason of the lower limit, $m_{1/2} > 2$ TeV, clearly visible in Figs. 4, 5 (the bino mass is approximately half the initial gaugino mass at M_X).

Although the prospects of LHC to discover or discard this scenario are clearly pessimistic, future XENON measurements could do the job. In fig. 6 we display the 2D joint posterior pdf of the spin–independent scattering cross section of a neutralino off a proton versus the neutralino mass for log priors and both signs of μ. As expected from the previous discussion, the posterior pdf of the neutralino masses is confined around 1 TeV. In contrast, the spin-independent scattering cross section covers several orders of magnitude. The present XENON100 and future XENON1T limits are also indicated in the plots. Clearly, most of the significant region favoured at the 95 % level will be within reach of the next generation of direct detection experiments, which are certainly good news for the CMSSM.

Let us finally notice the fact, that, contrary to what happened before including DM constraints, the pdf in A_0 shows a clear trend towards positive values. This has to do with the Focus-point regime. If A_0 is negative, its absolute value at low-energy increases. This increase is translates to the running of $m_{H_u}^2$, which becomes more negative at low-energy. As a consequence, the required value of μ^2 to achieve successful electroweak breaking increases. This implies a larger fine-tuning and makes more difficult the implementation of the Focus-Point solution to the DM abundance. For positive A_0, the behavior is the opposite. Without the DM constraints the Focus-Point area was already inside the preferred region, but it was not the only one, as can be seen from fig. 2, thus the two signs of A_0 had approximately the same statistical weight.

Multi-Component DM

Relaxing the requirement that all of the DM is made of LSPs implies that the WMAP measurement is just an upper bound on its abundance. At it is shown in the Appendix of ref. [76], in this case, the correct effective likelihood is given by the expression

$$\mathcal{L}_{\rm WMAP}(\Omega_{\rm LSP}h^2) = \mathcal{L}_0 \int_{\Omega_{\rm LSP}h^2/\sigma_{\rm WMAP}}^{\infty} e^{-\frac{1}{2}(x-r_\star)} x^{-1} {\rm d}x, \tag{4.2}$$

where $\mathcal{L}_0$ is an irrelevant normalization constant, $r_\star \equiv \mu_{\rm WMAP}/\sigma_{\rm WMAP}$ and $\Omega_{\rm LSP}h^2$ is the predicted relic density of the LSP as a function of the CMSSM and SM parameters.

When the LSP is not the only constituent of DM, the rate of events in a direct-detection experiment is smaller, since it is proportional to the local density of the LSP, ρ_χ, which is now smaller than the total local DM density, $\rho_{\rm DM}$. The suppression is given by the factor $\xi \equiv \rho_\chi/\rho_{\rm DM}$. Following ref. [77], we assume that ratio of local LSP and total DM densities is equal to that for the cosmic abundances, thus $\xi \equiv \rho_\chi/\rho_{\rm DM} = \Omega_\chi/\Omega_{\rm DM}$. For $\Omega_{\rm DM}$ we adopt the central value of the WMAP determination see Table 2, while for $\rho_{\rm DM}$ we adopt, following ref. [72], the value $0.4\,{\rm GeV\,cm^{-3}}$. This allows to evaluate ξ for each point in the CMSSM parameter space.

The effect of allowing a multi-component DM in the 1D posterior pdfs is displayed in Figs. 7, 8, which should be compared with the previous Figs. 4, 5, when the LSP was assumed to be the only component of DM. The most notable effect is that now large areas with lighter $m_{1/2}$ are recovered. This is easy to understand. As mentioned above, if the neutralino is pure Higgsino, for $m_\chi < 1$ TeV, the LSP abundance is less than the observed DM abundance. This does not represent now any problem, as one assumes that the DM has other components. Hence, smaller values of m_χ, or equivalently of μ, are now rescued. The condition for the Higgsino to be the LSP is that the bino mass is not smaller than μ. Consequently, $m_{1/2}$ (and thus $m_{\tilde{g}}$) can now be smaller, as reflected in Figs. 7, 8. On the other hand, it is now possible for $m_{1/2}$ to go even below that limit. The reason is that, although in that case the neutralino becomes a mixture of Higgsino and bino, which is potentially dangerous from XENON limits, the rescaling factor ξ reduces the predicted signal of recoil events. The actual value of ξ depends on the neutralino mass and the composition of the mixture.

The effect of all this is to bring $m_{1/2}$ to lower values, leading to gluino and squark masses of $\mathcal{O}(1)$ TeV within the LHC reach. This can be seen in the lower panel of fig. 7. Therefore we conclude that, regarding LHC searches, there are much better detection prospects in the case of multi-component DM than in the single-component DM scenario.

Finally, in fig. 9 we show the probability in the $(m_{\tilde{\chi}_1^0}, \sigma_p^{\rm SI})$ plane. The shape of the distribution is easy to understand from the above discussion. Neutralino masses of $\mathcal{O}(100)$ GeV become now allowed at the 95 % Bayesian credibility level, though the upper bound remains at of ~ 1 TeV. In addition, values of $\sigma_p^{\rm SI} > 10^{-8}$ pb are now within the 95 % level due to the suppresion caused by the ξ factor in predicted recoil events signal. The XENON1T expected 90 % exclusion limit contour is also displayed, showing that the

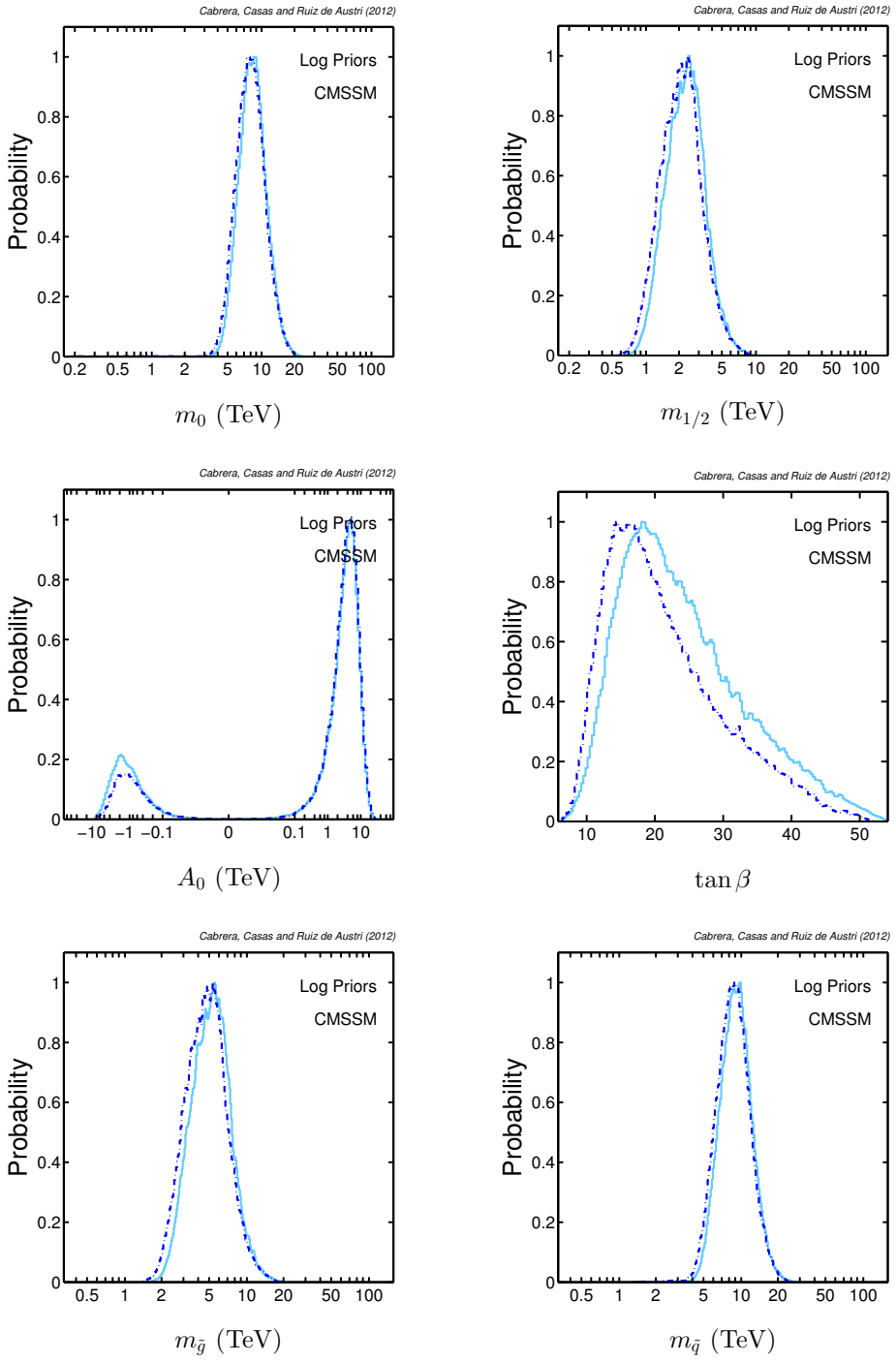

Figure 7: As in fig. 4 but considering that the LSP is not the soley DM component.

region favored by the data at the 95 % level can be fully probed by future tone-scale direct detection experiments.

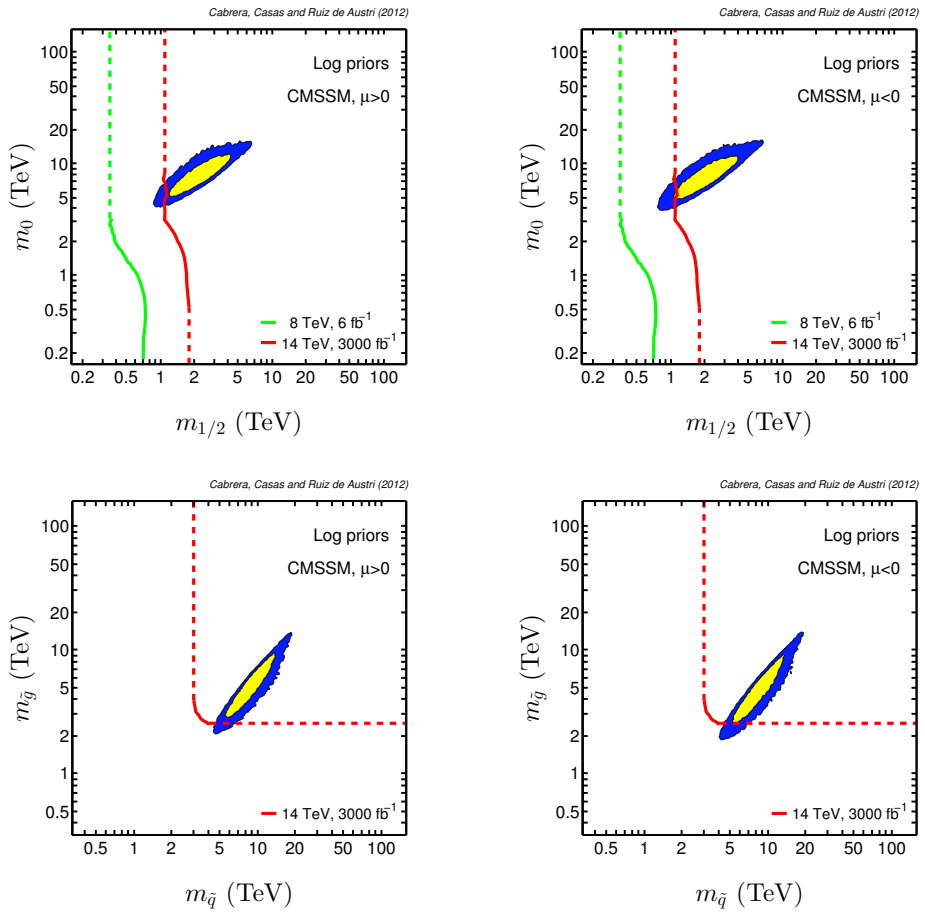

Figure 8: As in fig. 5 but considering that the LSP is not the soley DM component.

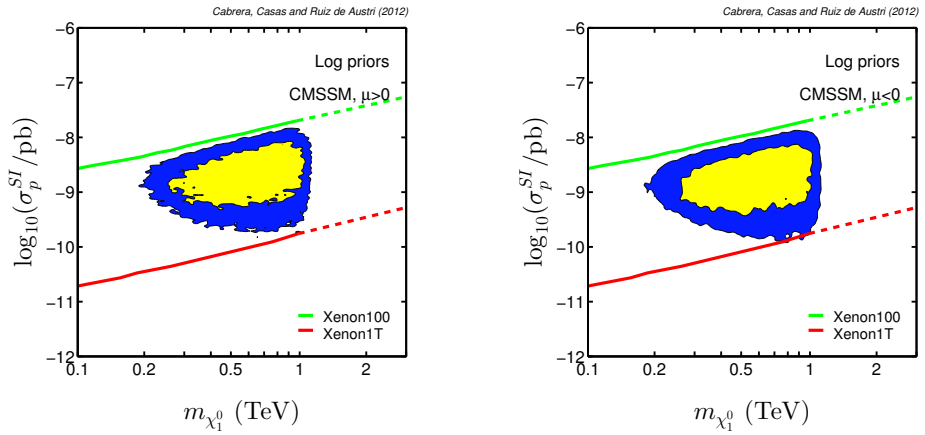

Figure 9: As in fig. 6 but considering that the LSP is not the soley DM component.

4.3 g-2

The magnetic anomaly of the muon, $a_\mu = \frac{1}{2}(g-2)_\mu$ has been a classical and powerful test

for new physics. The theoretical determination of a_μ depends crucially on the evaluation of the contribution coming from the hadronic vacuum-polarization diagram. This can be expressed in terms of the total hadronic cross section $e^+e^- \to$ had or, alternatively, in terms of the hadronic $\tau-$decay data, which are theoretically related to the e^+e^- hadronic cross section. Both approaches lead to different results, although in the last times they have notably converged. On the other hand, in either case the results are in remarkable disagreement with the experimental determination. More precisely, defining $\delta a_\mu = \delta^{\rm exp} a_\mu - \delta^{\rm SM} a_\mu$, the recent results are $\delta a_\mu = (25.5 \pm 8.0) \times 10^{-10}$ (using e^+e^- data) and $\delta a_\mu = (15.7 \pm 8.2) \times 10^{-10}$ (using $\tau-$decay data) [78, 79]. This corresponds to a discrepancy of 3.2σ and 1.9σ respectively.

This potential signal of new physics may be attributed to supersymmetric contributions to the muon anomaly, $\delta^{\rm MSSM} a_\mu$, which arise mainly from 1-loop diagrams with chargino or neutralino exchange [80, 81, 82, 83, 84]. This contribution i ncreases with increasing $\tan\beta$ and decreasing supersymmetric masses. The problem is that the large Higgs mass revealed by the experiment, well above M_Z, requires large supersymmetric masses, which is hardly conciliable with a sizeable $\delta^{\rm MSSM} a_\mu$. This is the reason why we have not used the $g-2$ result in the computation of the likelihood in our analysis. Besides, the $g-2$ computation has been rather controversial in the last years and probably the situation is not clear enough yet.

The Bayesian approach allows for a quantification of the discrepancy between the observed Higgs mass and the assumption that the supersymmetric contributions are responsible for δa_μ. We briefly describe the procedure (for more details see ref.[85, 86, 87]), which will also be used in sect.6 in other context. The idea is to separate the complete set of data in two subsets:

$$\{\text{data}\} = \{\mathscr{D}, D\} \tag{4.3}$$

Here $\mathscr{D}$ represents the subset of observations, whose compatibity with the rest of the observations, D, we want to test. In our case, $\mathscr{D}$ is the experimental value of a_μ, whereas D denotes the remaining experimental data, including the experimental Higgs mass. Then one constructs the quantity $p(\mathscr{D}|D)$, i.e. the probability of getting a certain result when measuring $\mathscr{D} \equiv a_\mu$, given the known values of the remaining observables,

$$p(\mathscr{D}|D) \;=\; \frac{p(\mathscr{D}, D)}{p(D)} \tag{4.4}$$

Here $p(\mathscr{D}, D)$ is probability of measuring both sets of data at the same time, while $p(D)$ is the analogue, but just for the D subset. These probabilities are given by the integral of the likelihood times the prior in the parameter space, and therefore coincide with the normalization factor appearing in denominator of eq.(2.2), sometimes called the *evidence*. E.g.

$$p(\mathscr{D}, D) = p(\text{data}) \;=\; \int d\theta_1 \cdots\; d\theta_N \; p(\text{data}|\theta_i)\; p(\theta_i)\;. \tag{4.5}$$

Now, the consistency of $\mathscr{D}^{\rm obs}$ (i.e. the actually measured muon anomaly) with the rest of data, D, can be tested by comparing the probability $p(\mathscr{D}^{\rm obs}|D)$ with the one obtained for the value of $\mathscr{D}$ that maximizes such probability, say $\mathscr{D}^{\rm max}$ (assuming the same reported error at the new central value). $\mathscr{D}^{\rm max}$ is somehow the "prediction" of the model for the muon anomaly, given the rest of experimental data. The quantity

$$\mathscr{L}(\mathscr{D}^{\rm obs}|D) \equiv \frac{p(\mathscr{D}^{\rm obs}|D)}{p(\mathscr{D}^{\rm max}|D)} = \frac{p(\mathscr{D}^{\rm obs},D)}{p(\mathscr{D}^{\rm max},D)} \tag{4.6}$$

is a global likelihood ratio (integrated to all possible values of the parameters of the model). Note that the $p(D)$ factor cancels out in the expression of $\mathscr{L}(\mathscr{D}^{\rm obs}|D)$, which is simply given by the ratio of the global evidences. This was called the $\mathscr{L}-$test in ref.[87]. If this likelihhod has a Gaussian-like profile, the quantity $-2\ln\mathscr{L}(\mathscr{D}^{\rm obs}|D)$ can be interpreted as $\sigma-$deviation from the theoretical prediction.

Obviously, for very large m_h, the supersymmetric particles must be very heavy. In that limit SUSY decouples, so $\mathscr{D}^{\rm max}$ should approach the SM prediction, i.e. $-2\ln\mathscr{L}(\mathscr{D}^{\rm obs}|D) \to 3.2^2$ (asuming the theoretical calculation of a_μ based on e^+e^- data); which is indeed the case [88]. Now, one can compute $\mathscr{L}$ for any value of m_h, in particular for $m_h = 125.9 \pm 0.4$ GeV, as given by the experiment. Our calculation indicates that, essentially, for this value of the Higgs mass, $\mathscr{L}$ has already reached its maximum (decoupling limit) value. In other words, the tension between the experimental Higgs mass and the experimental a_μ is already as large as for the SM (and thus larger than 3σ). This means that in the regions of the CMSSM where the prediction for a_μ is closer to the experiment than the SM prediction are not favoured since they present an onerous disagreement with t he observed Higgs mass. In some tiny regions this price can be somewhat alleviated, but they are statistically quite irrelevant, which reflects the cost of the underlying fine-tuning.

5. NUHM

Let us now (more briefly) describe the results when the MSSM model considered is the Non Universal Higgs Masses one (NUHM). Most of the discussion (and many of the results) are in fact analogous and it is not necessary to repeat them here. Hence, we will focus on the new features and their origin.

A slight difference has to do with the choice of the priors. Actually, the priors we have used for the NUHM are the same as the ones described in eq. (2.14) - (2.18), but now we have to include the common mass for the Higgses at M_X, i.e. m_H as an additional independent parameter. Then, the log prior reads,

$$p(m_0, m_H, m_{1/2}, A, B, \mu) \propto \frac{1}{[\max\{m_0, m_H, m_{1/2}, |A|, |B|, \mu, M_S^0\}]^6}, \tag{5.1}$$

and the flat prior,

$$p(m_0, m_H, m_{1/2}, A, B, \mu) \propto \frac{1}{[\max\{m_0, m_H, m_{1/2}, |A|, |B|, \mu, M_S^0\}]^4}. \tag{5.2}$$

Figs. 10, 11 show the results when DM constraints are not included in the analysis. They are analogous to Figs. 1, 2 for the CMSSM. Fig. 10 shows the posterior probability distribution function for m_0, m_H, $m_{1/2}$, A_0 and $\tan\beta$, for log and flat priors and $\mu > 0$. The results for $\mu < 0$ are quite similar and are not shown. As in the CMSSM, the preferred region is in the high-energy region, mainly due to the large value of the Higgs mass. From the m_0 and m_H pdfs in fig. 10 or from the two-dimensional pdf in the $m_H - m_0$ plane in fig. 11 it is clear that the NUHM naturally prefers $m_0 < m_H$. The reason is that, as discussed in the Appendix, the separation of the m_0 and m_H values can be used to decrease the value of m_0 at which μ^2 becomes very small (and eventually negative). Recall that in the CMSSM this occurred for large m_0, and corresponded to the region of high m_0 in fig. 2. Actually, after including DM constraints, that "Focus-Point" region was the only surviving one. Now, it is possible (and pays) to live with smaller m_0, which statistically is advantageous. This is the origin of the low$-m_0$ region in Figs. 10, 11.

Finally, Figs. 12, 13 show the results after including DM constraints (assuming that the DM is purely LSP). The results are quite similar to those for the CMSSM, but shifted to the low-m_0 region for the above-commented reasons. The same happens if we allow multi-component DM (we do not show the plots to avoid proliferation of figures).

In general, the results for the NUHM are similar to those of the CMSSM, but preferring lower values of m_0, which slightly improves the chances of detection at LHC.

6. Can still SUSY be natural? The impact of the Higgs discovery in the naturalness of SUSY

The results of sets. 4, 5 show that the CMSSM and NUHM scenarios require large supersymmetric masses, which challenges the natural coexistence of SUSY with the electroweak scale (the problem is actually quite general for the MSSM, as discussed below). There are more-or-less sophisticated criteria in the literature to quantify the amount of fine-tuning of a given model [89, 90, 91, 92, 93, 94, 95, 96, 97, 98]. However, the most rigorous and free-of-prejudice way to treat the fine-tuning is precisely through the Bayesian analysis, which automatically incorporates a fine-tuning penalization, encoded in the Jacobian factor of eqs.(2.11, 2.13). On the other hand, it is important to note that a Bayesian analysis starts with the assumption that the scenario under consideration is the true one, and then it gives the regions of higher probability in the associated parameter space. It does not directly give a hint about the plausibility of the scenario, unless one establish a comparison with an al ternative one.

In spite of this, it is very interesting the fact that we can use the Bayesian approach to study how the plausibility of the MSSM has changed after the Higgs discovery, as we are about to see in this section. For that purpose we will use a similar strategy to the one followed in subsect.4.3. to study the tension posed by the $g-2$ data. As in that case, we separate the experimental data in two subsets

$$\{\text{data}\} = \{\mathscr{D}, D\} \tag{6.1}$$

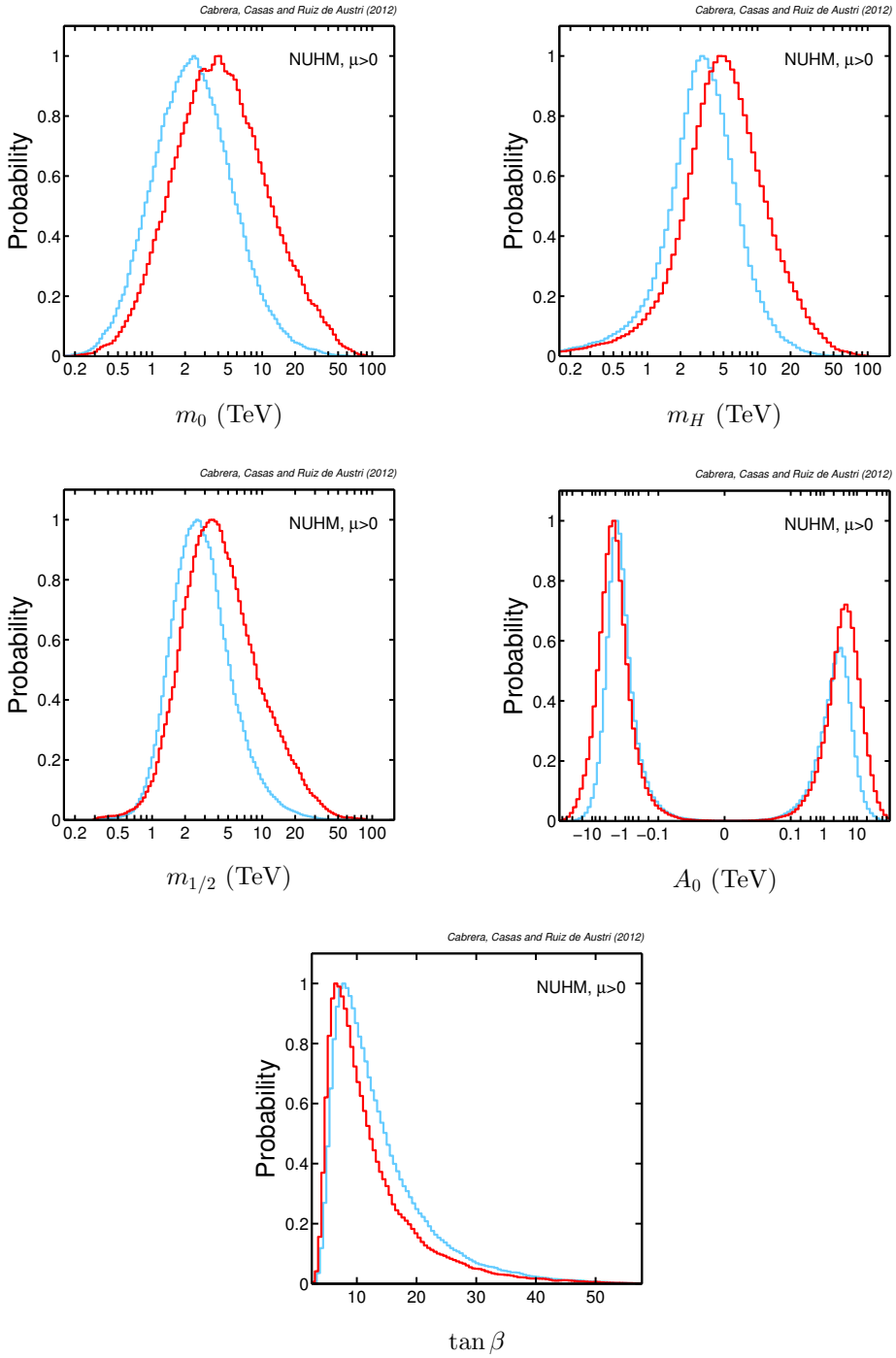

Figure 10: 1D marginalized posterior probability distribution of the NUHM parameters: $m_0, m_H, m_{1/2}, A$ and $\tan\beta$. The red(cyan) corresponds to flat(logarithmic) priors.

where $\mathcal{D}$ represents now the Higgs mass data and D the rest of experimental information.

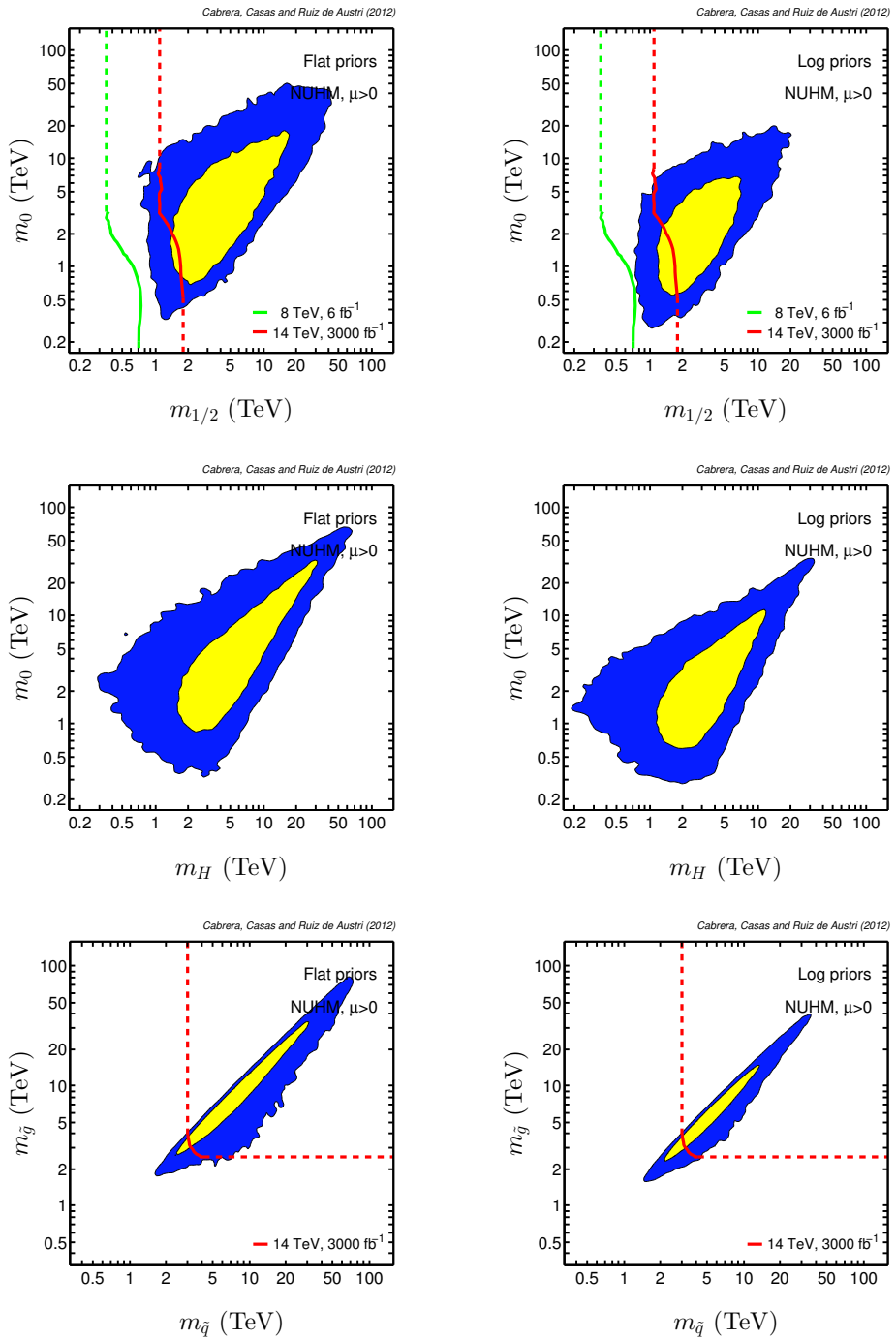

Figure 11: 2D marginalized posterior probability distribution of the NUHM in $m_{1/2}-m_0$, m_H-m_0 and $m_{\tilde{g}}-m_{\tilde{q}}$ planes. Left panels show the flat priors case and right panels the logarithmic one. The inner and outer contours enclose respective 68% and 95% joint regions.

As explained in subsect. 4.3 we construct now the $\mathscr{L}-$parameter, defined by

$$\mathscr{L}(\mathscr{D}^{\rm obs}|D) \equiv \frac{p(\mathscr{D}^{\rm obs}|D)}{p(\mathscr{D}^{\rm max}|D)} = \frac{p(\mathscr{D}^{\rm obs},D)}{p(\mathscr{D}^{\rm max},D)} \tag{6.2}$$

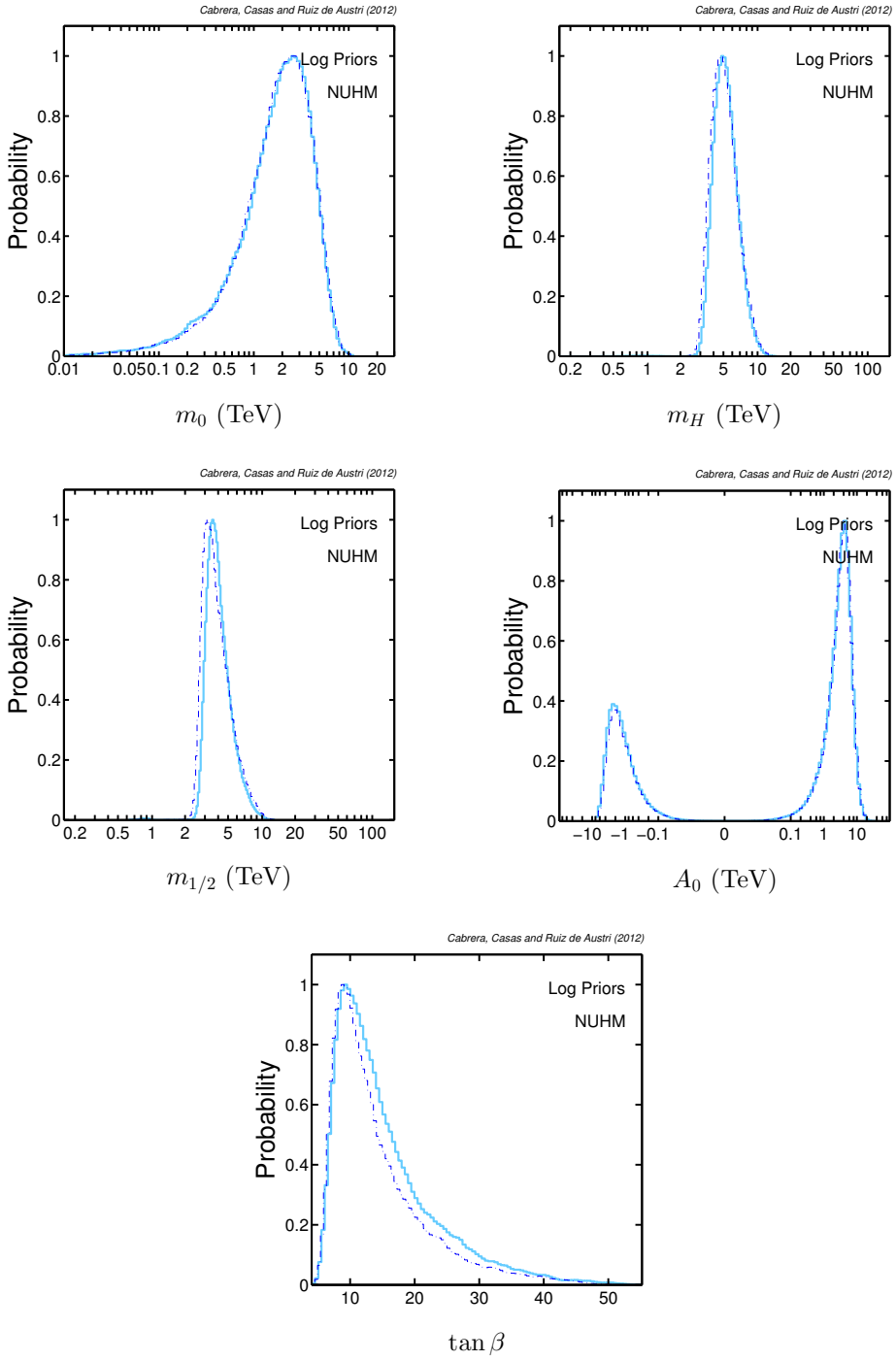

Figure 12: As in fig. 10 but with an additional constraint from DM (WMAP 7-years and XENON100) considering that the LSP is the soley DM component. Here the cyan line corresponds to a positive μ whereas the blue dashed to a negative μ.

Here $\mathscr{D}^{\max}$ is the would-have-been most probable value of the Higgs mass in the MSSM context, given the values of the other experimental data. Our analysis shows that, restrict-

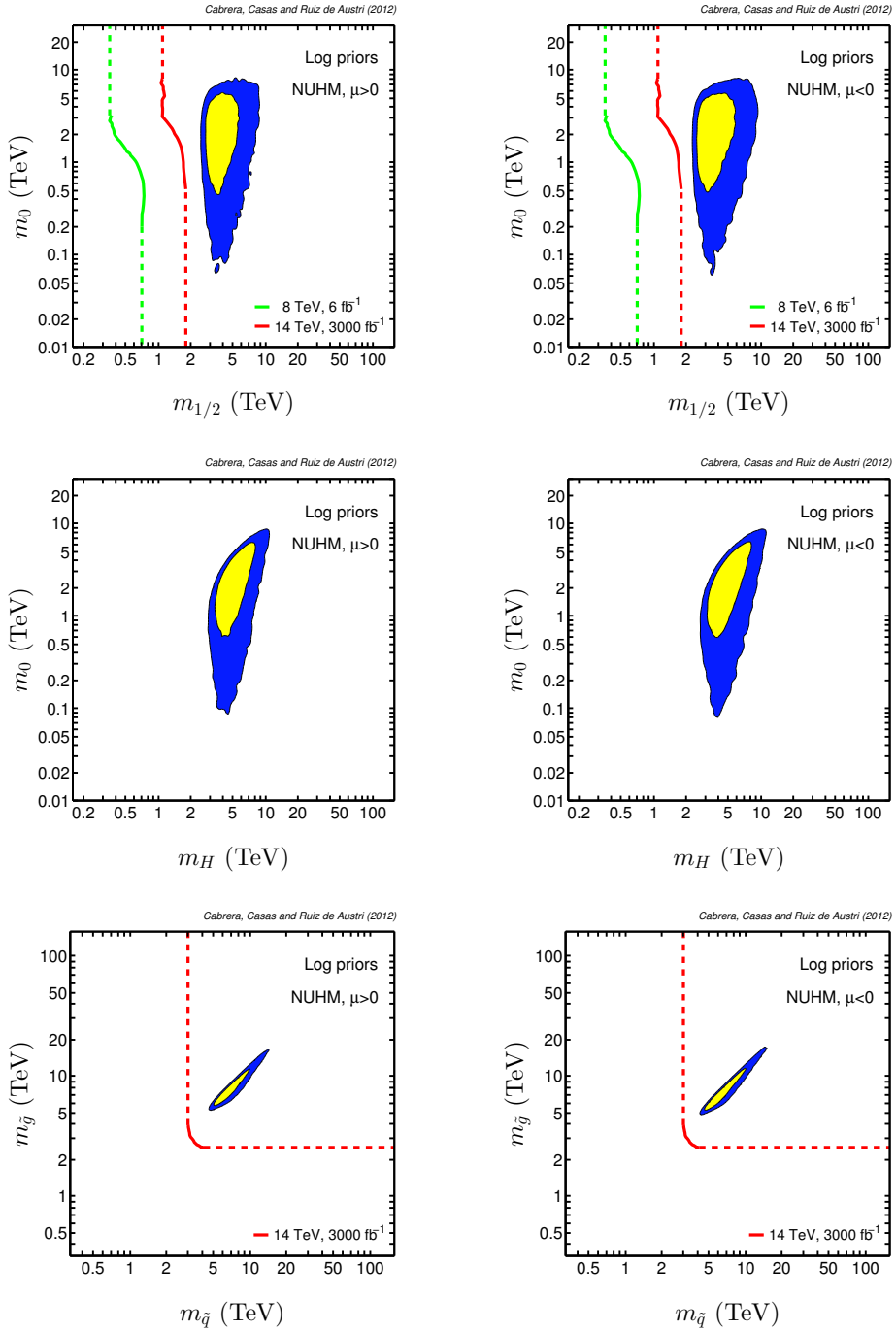

Figure 13: As in fig. 11 but with an additional constraint from DM (WMAP 7-years and XENON100) considering that the LSP is the soley DM component.

ing ourselves to the CMSSM scenario, this maximizing value is $m_h \simeq 117$ GeV. In other words this would have been the central value of the CMSSM 'prediction" for m_h just before the LHC discovery. This can also be seen from ref. [27]. Then the $\mathscr{L}-$parameter defined above gives the relative global likelihood of the actually measured m_h with respect to the

maximal one. The results of our computation of $\mathscr{L}$ are

$$\begin{aligned} \ln \mathscr{L} &= -1.92 \qquad \text{(log priors)} \\ \ln \mathscr{L} &= -0.70 \qquad \text{(flat priors)} \end{aligned} \tag{6.3}$$

which correspond to 1.9σ and 1.18σ respectively. (For this computation we have not included dark matter constraints.) The previous results show that, although the experimental Higgs mass is not certainly the preferred value in the CMSSM context, it is not as improbable as it would seem. This is in part due to the fact that an important CMSSM region, from the point of view of statistical weight, is the Focus-Point one. This region corresponds to large scalar masses (but with low fine-tuning due to the small value of μ) and thus to naturally large Higgs mass. The results for the NUHM are similar.

One can summarize this statement by saying that the experimental value of the Higgs mass is at $\sim 2\ \sigma$ off the supersymmetric predicted central value. Certainly, as past experiences showed, a $2\ \sigma$ discrepancy is not particularly dramatic and physicists are hardly impressed by it. Notice however, that this implies that, if the CMSSM is true, it lies in the $\sim 5\%$ less probable region, which is roughly consistent with the estimates in the literature that the 'supersymmetric fine-tuning is of a few percent".

So the conclusion is that, although the CMSSM or the NUHM are quite unlikely to show up at the LHC (at least using the present strategies to find out SUSY), they are still interesting and plausible models after the Higgs discovery. Let us say they are at $\sim 2\ \sigma$.

Finally, we would like to address a question related to the naturalness of SUSY, namely: To which extent the problems of the CMSSM and NUHM remain in general MSSMs? To address this question, let us recall that the original motivations for the CMSSM are 1) Minimal Flavour and CP violation, 2) Simplicity, 3) The fact that it arises in some theoretically motivated scenarios (like minimal SUGRA or Dilaton-dominated SUSY breaking). From these motivations only the first one is robust, but the experimental results do not require completely universal soft terms. E.g. the third generation of squarks and sleptons could have very different masses. The degeneracy of gaugino masses at M_X is not experimentally justified either. Therefore, going beyond the CMSSM (or the NUHM) is very plausible. Does this solve the problems of the CMSSM?

This question can be explored by promoting the CMSSM to more general MSSMs compatible with the flavour and CP constraints. Playing with the initial parameters it is possible to have a lighter third generation, as invoked in "natural SUSY" models. It also allows certain types of supersymmetric spectrum that can evade the detection at LHC. In particular if the LSP is heavy or the masses of the supersymmetric states are not far from each other ("compressed spectrum" [99]), then the supersymmetric events have small p_Ts and are triggered out in the experimental analyses. It is undoubtedly possible to arrange the MSSM spectrum in these ways in order to fool the LHC. But, in the absence of a solid theoretical reason for them, it sounds a rather artificial possibility.

In any case, in *any* MSSM the third generation cannot be too light, since it is needed to be rather heavy in order to reproduce (thanks to the radiative corrections) the experimental

mass of the Higgs. This requirement is alleviated if X_t is close to its maximizing value, but still the required stop masses imply that the electroweak breaking is quite fine-tuned, although perhaps not as much as it is often said, as we have discussed in this section. This situation could only improve substantially if one goes *beyond* the MSSM, which are out of the scope of this paper.

7. Comparison with previous literature

There are several works in the literature that have incorporated the impact of a Higgs at $\sim$ 125 GeV and/or the new XENON100 data into Bayesian and frequentist analyses [6, 7, 8, 11, 9]. Some of them are previous to the announcement of the Higgs discovery, and thus have a slightly different central value and uncertainty of m_h from that reported in ref.[1, 2]. However, that departure is not dramatic, even though small shifts in the Higgs mass have an important effect in the SUSY studies, as is clear e.g. from the discussion in sect. 4. On the other hand, there are important differences between the approaches followed in the various analyses and the results obtained in them. The aim of this section is to show the consistency of all the results, to explain the origin of the discrepancies and to argue what are the most reliable results and conclusions.

Let us start with other Bayesian studies of the CMSSM and/or the NUHM after the Higgs discovery, namely those of refs.[7, 8, 11]. One can check that, in spite of being based on more or less the same data, the results do not look the same (compared with each other and with the present paper). To be more concrete, consider the probability distribution function in the $m_{1/2} - m_0$ plane in the CMSSM with $\mu > 0$, using log priors and including the DM constraints. In ref.[8] they allow for multi-component DM, so the top-left plot of their figure 1 must be compared to the top-left plot of our fig. 8. Actually, they are quite consistent (the preferred region is in the area of the Focus-Point), although the plot of ref.[8] is cut at 8 TeV and does not show most of the allowed region visible in our fig. 8. This cut is not an artifact of the representation, but the actual upper limit considered for m_0 in ref.[8]. But otherwise, the results are in very good agreement. On the other hand, the left plot of figure 2 of ref.[7] and the first plot in the middle row of figure 4 of ref.[11] correspond to the requirement that the DM is supersymmetric. Hence, they should be compared with the top-left plot of our fig. 5. Actually, the plots of those two references are quite consistent with each other, but they show a preferred region, with quite small soft masses, which does *not* show up at all, neither in our plot nor in the plot of ref.[8] (which being less restrictive should display it). What is going on?

The origin of these discrepancies lies on the different ranges used for the soft parameters. Not only one can leave aside a most interesting region if the ranges are too restrictive. In addition, as discussed after eq.(2.3), the results obtained by marginalizing the non-shown parameters may depend on the ranges of integration. The upper-limits of the ranges for $(m_0, m_{1/2})$ in refs. [8, 7, 11] were (8 TeV, 5 TeV), (4TeV, 2 TeV) and (4 TeV, 4 TeV). This explains why the latter two references missed the region where the bulk of the probability is (the Focus-Point) and show only the less satisfactory stau-coannihilation and $A-$funnel

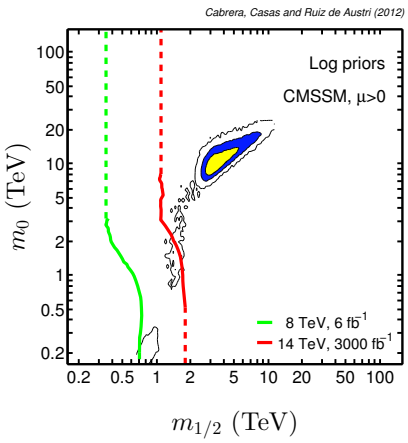

Figure 14: 2D marginalized posterior probability distribution of the CMSSM in the $m_{1/2}$–m_0 plane, using log priors and DM constraints. The yellow and blue areas enclose respective 68% and 95% joint regions. The white one corresponds to 99.9% c.l.

regions. As discussed in subject. 4.2 these two regions are disfavored, as they corresponds to rather small soft terms, difficult to reconcile with the Higgs mass (they are still consistent thanks to the theoretical uncertainty assumed in the supersymmetric calculation). This is why these regions do not belong to the 68% and 95% c. l. regions in the plots of ref. [8] and the present paper. In fact, one can force these two regions to appear by plotting the contours of higher confidence levels. We have checked that they become visible for the 99.9% c.l. region, as fig. 14 shows. The new contours are consistent with those shown in refs. [7, 11], but they are extremely disfavored.

The conclusion here is that it is very convenient to use an approach that makes the actual ranges for the parameters irrelevant. This is in fact possible, taking profit of the Jacobian factor discussed in sect. 2, which penalizes fine-tuned regions at high scale. In this sense, we honestly think that the results presented here are very reliable and represent an improvement with respect to previous analyses.

Let us finally comment briefly on frequentist approaches. These are based on the analysis of the likelihood function in the parameter space. The scan of the parameter space, evaluating the likelihood based on the χ^2, leads to zones of estimated probability (inside contours of constant χ^2) around the best fit points. In doing so, the unplotted variables are optimized to obtain the best χ^2. Two recent frequentist analyses incorporating a Higgs mass at 125 GeV are those of ref. [9] and ref. [11] (the first one was made before the Higgs discovery). They are quite consistent with each other, obtaining a best-fit point in the stau-coannihilation region. The preferred areas are inside this region and in the $A-$funnel one. Roughly speaking, they coincide with those obtained in the Bayesian analyses of refs.[7, 11]. The fact that the Focus-Point region with pure Higgsino LSP does not appear is probably a consequence of the limited ranges used in the scan of $m_{1/2}, m_0$. In addition, a frequentist analysis is not sensitive to the fine-tuning. Fine-tuning has to do with statistical weight and a frequentist analysis is based entirely on likelihood, i.e. the ability to reproduce

the experiment, and thus cannot "see" the fine-tuning. E.g. a point (o a region) in the parameter space can present an optimal likelihood, but only after an extreme tuning of the unplotted parameters. This feature makes this point extremely unplausible (even if it is capable to reproduce the experimental data), but this does not affect its privileged condition in a frequentist approach. This fact can favor points in the low-energy regions, which are suppressed in the Bayesian approach.

8. Conclusions

The most obvious conclusion from the results presented in this paper is that *if* the CMSSM or the NUHM are the model chosen by nature, the Bayesian analysis shows that they probably live in a region of the parameter space of large supersymmetric masses (squark and gluino masses above ~ 2 TeV), which makes very problematic their discovery at LHC. The quite large Higgs mass, $m_h \simeq 126$ GeV, is the main responsible for these negative results. Actually, given the experimental value of m_h, it would have been extremely improbable that the LHC had already detected a signal of new physics corresponding to the CMSSM or the NUHM. The Higgs mass is more powerful than the direct detection limits in pushing the MSSM parameter space into the large-energy region. Actually, we will be quite lucky if one of these models is correct *and* is still detectable in the next years, at least with the current techniques to look for physics beyond the SM at the LHC. We have quantified these probabilities with a rigorous and improved Bayesian analysis, whose results are remarkably independent of the choice of the priors and of the ranges assumed for the independent parameters.

The previous conclusion is even more dramatic if one includes dark matter constraints in the analysis, in particular the last XENON100 data. These are able to discard a large portion of the Focus-Point region, while other regions (co-annihilation and $A-$funnel) are very disfavored from the experimental Higgs mass. There survives a fraction of the Focus-Point region with large scalar and gaugino masses, where the LSP neutralino is almost pure Higgsino. Its mass is constrained to be quite close to 1 TeV. This extreme conclusion is relaxed if one allows the dark matter to have other components (e.g. axions). Then a large part of the Focus-Point region is rescued. Interestingly, the future XENON1T data will be able to test these regions. Therefore, if the CMSSM or the NUHM are the true models of nature, it is more plausible to discover them in experiments of direct-detection of dark matter than in the LHC.

Our Bayesian analysis contains an automatic (non-imposed) penalization of fine-tuned regions. This penalization arises from the Bayesian analysis itself when the value of M_Z is treated on the same foot as the rest of the experimental information (and not as a constraint of the model). This fine-tuning penalization is encoded in a model-independent Jacobian factor, which should never be ignored. This factor is also the responsible for the great stability against changes in the ranges of the parameters. We have shown that the different choices made for these ranges in previous analyses (which did not include the Jacobian penalization) have led to apparent discrepancies between the results obtained by

different groups. We demonstrate that all of them are consistent once the freedom in the ranges is taken into account. This has motivated also that some previous analyses have missed important regions in the supersymmetric parameter space.

Although the 125 GeV Higgs pushes SUSY to regions where is hardly detectable at the LHC, this does not necessarily mean that SUSY is very fine-tuned. Actually, the Focus-Point region is not particularly fine-tuned, despite having large supersymmetric masses, since the value of μ is small. In this paper we have evaluated to which extent the Higgs discovery has diminished the naturalness of SUSY (focussing on the CMSSM for this exercise). It is important to note that a Bayesian analysis starts with the assumption that the scenario under consideration is the true one, and then it gives the regions of higher probability in the associated parameter space. It does not directly give a hint about the plausibility of the scenario, unless one establish a comparison with an alternative one. Still, it is remarkable that we can use the Bayesian approach to study how the plausibility of the MSSM has changed after the Higgs discovery. The key is to perform the same Bayesian analysis with the same data except the Higgs mass, say as if we were in the year 2011. Then one obtains a preferred value for the Higgs mass (namely, around 117 GeV) with a probability profile; and one can compute how far apart from this prediction the actual experimental value is. This can be done with the help of Bayesian tecnhiques (comparing the evidence for different values of m_h). The result is that the Higgs mass is at $\sim 2\ \sigma$ off the supersymmetric predicted central value. Certainly, as past experiences showed, a $2\ \sigma$ discrepancy is not particularly dramatic and physicists are hardly impressed by it. Notice however, that this implies that, if the CMSSM is true, it lies in the $\sim 5\%$ less probable region, which is roughly consistent with the estimates in the literature that the 'supersymmetric fine-tuning is of a few percent".

So the final conclusion is that, although the CMSSM or the NUHM are quite unlikely to show up at the LHC (at least using the present strategies to find out SUSY), they are still interesting and plausible models after the Higgs discovery; and the chances of discovering them in future experiments of direct detection of dark matter are quite high.

A. Focus-Point behavior in the CMSSM and the NUHM

As first noticed by Feng et al [100], the focus point is a scale at which, for fixed $m_{1/2}$, m_0, A_0 and $\tan\beta$ in the CMSSM, the H_u mass, $m^2_{H_u}$, does not depend on the initial (high-energy) value of m_0. The value of that scale, which denote $Q_{\rm FP}$, depends mainly on the top yukawa and thus on $\tan\beta$. Surprisingly $Q_{\rm FP} \simeq M_Z$.

Let us now consider the required value of μ to obtain a correct electroweak breaking. First notice that from the minimization of the (tree-level) scalar potential, one gets

$$\mu^2 = \frac{m^2_{H_d} - m^2_{H_u}\tan^2\beta}{\tan^2\beta - 1} - \frac{1}{2}M_Z^2, \tag{A.1}$$

Therefore, for large values of $\tan\beta$ ($\gtrsim 8$) ,

$$\mu^2 \simeq -m^2_{H_u}. \tag{A.2}$$

Consequently if we are in a regime where $m^2_{H_u}$ is small at low-energy and $\tan\beta \gtrsim 8$, then the value of μ will also be small. [The precise value of $m^2_{H_u}$ depends on the CMSSM parameters (m_0, $m_{1/2}$, A_0, $\tan\beta$).] All this has important implications for the amount of fine-tuning (the smaller μ, the less fine-tuning) and for dark matter (if μ is small the lightest neutralino is mostly Higgsino, and the second neutralino and the lightest chargino are quasi-degenerate). On the other hand, the scale at which the electroweak breaking is evaluated, say $Q_{\rm EW}$, does not coincide exactly with M_Z (and thus with $Q_{\rm FP}$). Rather, it is given by an average of the stop masses, which is larger than M_Z. The actual value of $m^2_{H_u}$ at $Q_{\rm EW}$ is given by the running from $Q_{\rm FP}$ to $Q_{\rm EW}$. This represents a positive shift. Since $m^2_{H_u}$ is normally negative at low energy, its absolute value decreases. And from eq.(A.2), the value of μ^2 decreases too. This is interesting, but if $Q_{\rm FP}$ is too high (which typically occurs for large $m_{1/2}$ and/or m_0), μ^2 becomes negative. This means that there is no solution for the electroweak breaking. This puts upper limits on the values of $m_{1/2}$ and m_0 (more precisely on a certain combination of them). Near that limit μ^2 is small and we can have a pure Higgsino LSP. This is the CMSSM region favored in the Bayesian analysis when one includes dark matter constraints. Notice that it takes place for large $m_{1/2}$ and m_0.

Let us now go to the NUHM. In this case, one has the freedom to vary m_0 and m_H at high energy in an independent way. One can check that if one leaves $m_H(M_X)$ fixed while increases (decreases) $m_0(M_X)$, then the value of $m^2_{H_u}$ at low-energy will decrease (increase). Consequently, one can decrease the absolute value of $m^2_{H_u}$, and thus of μ^2, simply by going to a region in the parameter space where $m_0 < m_H$. This region is analogous to the Focus-Point region of the CMSSM; but now one can have smaller values of m_0, and thus of squark masses. Actually, the Bayesian analysis selects this region as the preferred one in the NUHM when dark matter constraints are included. This explains the (non-dramatic) differences between the CMSSM and the NUHM plots (e.g. Fig. 5 vs Fig. 18).

Acknowledgements. We would like to thank Roberto Trotta and Charlotte Strege for providing us with the Xenon100 likelihood implementation. R. RdA, is supported by the Ramón y Cajal program of the Spanish MICINN and also thanks the support of the Spanish MICINN's Consolider-Ingenio 2010 Programme under the grant MULTIDARK CSD2209-00064 and the Invisibles European ITN project (FP7-PEOPLE-2011-ITN, PITN-GA-2011-289442-INVISIBLES). The work of A. Casas has been partially supported by the MICINN, Spain, under contract FPA2010-17747 and the Consolider-Ingenio PAU CSD2007-00060, CPAN CSD2007-00042. We thank as well the Comunidad de Madrid through Proyecto HEPHACOS S2009/ESP-1473 and the European Commission under contract PITN-GA-2009-237920. M.E. Cabrera acknowledges the financial support of the CSIC through a predoctoral research grant (JAEPre 07 00020) and the ERC Starting *Grant WIMPs Kairos - the moment of truth for wimp dark matter?* (P.I. Gianfranco Bertone). The use of IFT-UAM High Performance Computing Service is gratefully acknowledged.

References

[1] **ATLAS** Collaboration, G. Aad *et. al.*, *Observation of a new particle in the search for the Standard Model Higgs boson with the ATLAS detector at the LHC*, *Phys.Lett.* **B716** (2012) 1–29 [1207.7214].

[2] **CMS** Collaboration, S. Chatrchyan *et. al.*, *Observation of a new boson at a mass of 125 GeV with the CMS experiment at the LHC*, *Phys.Lett.* **B716** (2012) 30–61 [1207.7235].

[3] *Updated atlas results on the signal strength of the higgs-like boson for decays into ww and heavy fermion final states*, Tech. Rep. ATLAS-CONF-2012-162, CERN, Geneva, Nov, 2012.

[4] *Combination of standard model higgs boson searches and measurements of the properties of the new boson with a mass near 125 gev*, .

[5] M. Farina, M. Kadastik, D. Pappadopulo, J. Pata, M. Raidal *et. al.*, *Implications of XENON100 and LHC results for Dark Matter models*, *Nucl.Phys.* **B853** (2011) 607–624 [1104.3572].

[6] C. Balazs, A. Buckley, D. Carter, B. Farmer and M. White, *Should we still believe in constrained supersymmetry?*, 1205.1568.

[7] A. Fowlie, M. Kazana, K. Kowalska, S. Munir, L. Roszkowski *et. al.*, *The CMSSM Favoring New Territories: The Impact of New LHC Limits and a 125 GeV Higgs*, *Phys.Rev.* **D86** (2012) 075010 [1206.0264].

[8] S. Akula, P. Nath and G. Peim, *Implications of the Higgs Boson Discovery for mSUGRA*, *Phys.Lett.* **B717** (2012) 188–192 [1207.1839].

[9] O. Buchmueller, R. Cavanaugh, M. Citron, A. De Roeck, M. Dolan *et. al.*, *The CMSSM and NUHM1 in Light of 7 TeV LHC, $B_s$tomu + mu− and XENON100 Data*, *Eur.Phys.J.* **C72** (2012) 2243 [1207.7315].

[10] A. Arbey, M. Battaglia, A. Djouadi and F. Mahmoudi, *The Higgs sector of the phenomenological MSSM in the light of the Higgs boson discovery*, *JHEP* **1209** (2012) 107 [1207.1348].

[11] C. Strege, G. Bertone, F. Feroz, M. Fornasa, R. R. de Austri *et. al.*, *Global Fits of the cMSSM and NUHM including the LHC Higgs discovery and new XENON100 constraints*, 1212.2636.

[12] M. E. Cabrera, J. A. Casas and R. Ruiz de Austri, *Bayesian approach and Naturalness in MSSM analyses for the LHC*, *JHEP* **03** (2009) 075 [0812.0536].

[13] A. Strumia, *Naturalness of supersymmetric models*, hep-ph/9904247. This paper is mainly a brief discussion of hep-ph 9911386, with only few original points.

[14] J. R. Ellis, K. Enqvist, D. V. Nanopoulos and F. Zwirner, *Observables in Low-Energy Superstring Models*, *Mod.Phys.Lett.* **A1** (1986) 57.

[15] R. Barbieri and G. Giudice, *Upper Bounds on Supersymmetric Particle Masses*, *Nucl.Phys.* **B306** (1988) 63.

[16] B. Allanach, *SOFTSUSY: a program for calculating supersymmetric spectra*, *Comput.Phys.Commun.* **143** (2002) 305–331 [hep-ph/0104145].

[17] B. M. Kastening, *Renormalization group improvement of the effective potential in massive phi**4 theory*, *Phys.Lett.* **B283** (1992) 287–292.

[18] C. Ford, D. Jones, P. Stephenson and M. Einhorn, *The Effective potential and the renormalization group*, *Nucl.Phys.* **B395** (1993) 17–34 [hep-lat/9210033].

[19] M. Bando, T. Kugo, N. Maekawa and H. Nakano, *Improving the effective potential*, *Phys.Lett.* **B301** (1993) 83–89 [hep-ph/9210228].

[20] J. A. Casas, J. R. Espinosa, M. Quiros and A. Riotto, *The Lightest Higgs boson mass in the minimal supersymmetric standard model*, *Nucl. Phys.* **B436** (1995) 3–29 [hep-ph/9407389].

[21] L. E. Ibanez and C. Lopez, *N=1 Supergravity, the Weak Scale and the Low-Energy Particle Spectrum*, *Nucl.Phys.* **B233** (1984) 511.

[22] L. J. Hall, R. Rattazzi and U. Sarid, *The Top quark mass in supersymmetric SO(10) unification*, *Phys.Rev.* **D50** (1994) 7048–7065 [hep-ph/9306309].

[23] A. E. Nelson and L. Randall, *Naturally large tan BETA*, *Phys.Lett.* **B316** (1993) 516–520 [hep-ph/9308277].

[24] V. S. Kaplunovsky and J. Louis, *Model independent analysis of soft terms in effective supergravity and in string theory*, *Phys.Lett.* **B306** (1993) 269–275 [hep-th/9303040].

[25] G. Giudice and A. Masiero, *A Natural Solution to the mu Problem in Supergravity Theories*, *Phys.Lett.* **B206** (1988) 480–484.

[26] B. C. Allanach, K. Cranmer, C. G. Lester and A. M. Weber, *Natural priors, CMSSM fits and LHC weather forecasts*, *JHEP* **0708** (2007) 023 [0705.0487].

[27] M. E. Cabrera, J. A. Casas and R. Ruiz d Austri, *MSSM Forecast for the LHC*, *JHEP* **05** (2010) 043 [0911.4686].

[28] **Tevatron Electroweak Working Group, CDF Collaboration, D0 Collaboration** Collaboration, *Combination of CDF and D0 results on the mass of the top quark using up to 5.8 fb-1 of data*, 1107.5255.

[29] **Particle Data Group** Collaboration, W. Yao *et. al.*, *Review of Particle Physics*, *J.Phys.* **G33** (2006) 1–1232.

[30] K. Hagiwara, A. Martin, D. Nomura and T. Teubner, *Improved predictions for g-2 of the muon and alpha(QED) (M**2(Z))*, *Phys.Lett.* **B649** (2007) 173–179 [hep-ph/0611102].

[31] R. R. de Austri, R. Trotta and L. Roszkowski, *A Markov chain Monte Carlo analysis of the CMSSM*, *JHEP* **0605** (2006) 002 [hep-ph/0602028].

[32] *http://lepewwg.web.cern.ch/LEPEWWG*.

[33] **Heavy Flavor Averaging Group** Collaboration, Y. Amhis *et. al.*, *Averages of b-hadron, c-hadron, and tau-lepton properties as of early 2012*, 1207.1158.

[34] **LHCb** Collaboration, R. Aaij *et. al.*, *Measurement of the $B_s^0 - \bar{B}_s^0$ oscillation frequency Δm_s in $B_s^0 \to D_s^-(3)\pi$ decays*, *Phys.Lett.* **B709** (2012) 177–184 [1112.4311].

[35] **BABAR** Collaboration, B. Aubert *et. al.*, *Measurement of Branching Fractions and CP and Isospin Asymmetries in $B \to K^*\gamma$*, 0808.1915.

[36] **BABAR** Collaboration, B. Aubert *et. al.*, *Observation of the semileptonic decays $B \to D^*\tau^-\bar{\nu}(\tau)$ and evidence for $B \to D\tau^-\bar{\nu}(\tau)$*, *Phys.Rev.Lett.* **100** (2008) 021801 [0709.1698].

[37] **FlaviaNet Working Group on Kaon Decays** Collaboration, M. Antonelli *et. al.*, *Precision tests of the Standard Model with leptonic and semileptonic kaon decays*, 0801.1817.

[38] **LHCb** Collaboration, R. Aaij *et. al.*, *First evidence for the decay $B_s \to \mu^+\mu^-$*, 1211.2674.

[39] N. Jarosik, C. Bennett, J. Dunkley, B. Gold, M. Greason *et. al.*, *Seven-Year Wilkinson Microwave Anisotropy Probe (WMAP) Observations: Sky Maps, Systematic Errors, and Basic Results*, *Astrophys.J.Suppl.* **192** (2011) 14 [1001.4744].

[40] *https://twiki.cern.ch/twiki/bin/view/CMSPublic/PhysicsResults*.

[41] *Search for squarks and gluinos with the atlas detector using final states with jets and missing transverse momentum and 5.8 fb^{-1} of $\sqrt{s}$=8 tev proton-proton collision data*, Tech. Rep. ATLAS-CONF-2012-109, CERN, Geneva, Aug, 2012.

[42] **CMS** Collaboration, *Search for neutral higgs bosons decaying into tau leptons in the dimuon channel with cms in pp collisions at 7 tev*, .

[43] **XENON100** Collaboration, E. Aprile *et. al.*, *Dark Matter Results from 225 Live Days of XENON100 Data*, *Phys.Rev.Lett.* **109** (2012) 181301 [1207.5988].

[44] A. Dedes, G. Degrassi and P. Slavich, *On the two loop Yukawa corrections to the MSSM Higgs boson masses at large tan beta*, *Nucl.Phys.* **B672** (2003) 144–162 [hep-ph/0305127].

[45] M. Awramik, M. Czakon, A. Freitas and G. Weiglein, *Precise prediction for the W boson mass in the standard model*, *Phys.Rev.* **D69** (2004) 053006 [hep-ph/0311148].

[46] M. Awramik, M. Czakon, A. Freitas and G. Weiglein, *Complete two-loop electroweak fermionic corrections to $\sin^2\theta^{\rm lept}_{\rm eff}$ and indirect determination of the Higgs boson mass*, *Phys.Rev.Lett.* **93** (2004) 201805 [hep-ph/0407317].

[47] A. Djouadi, P. Gambino, S. Heinemeyer, W. Hollik, C. Junger *et. al.*, *Leading QCD corrections to scalar quark contributions to electroweak precision observables*, *Phys.Rev.* **D57** (1998) 4179–4196 [hep-ph/9710438].

[48] G. Degrassi, P. Gambino and P. Slavich, *SusyBSG: A Fortran code for BR[$B \to X(s)\gamma$] in the MSSM with Minimal Flavor Violation*, *Comput.Phys.Commun.* **179** (2008) 759–771 [0712.3265].

[49] G. Degrassi, P. Gambino and P. Slavich, *QCD corrections to radiative B decays in the MSSM with minimal flavor violation*, *Phys.Lett.* **B635** (2006) 335–342 [hep-ph/0601135].

[50] G. D'Ambrosio, G. Giudice, G. Isidori and A. Strumia, *Minimal flavor violation: An Effective field theory approach*, *Nucl.Phys.* **B645** (2002) 155–187 [hep-ph/0207036].

[51] F. Mahmoudi, *SuperIso v2.3: A Program for calculating flavor physics observables in Supersymmetry*, *CPHCB,180,1579-1613.2009* **180** (2009) 1579–1613 [0808.3144].

[52] *http://superbayes.org*.

[53] **ATLAS** Collaboration, G. Aad *et. al.*, *Search for supersymmetry using final states with one lepton, jets, and missing transverse momentum with the ATLAS detector in $\sqrt{s} = 7$ TeV pp*, *Phys.Rev.Lett.* **106** (2011) 131802 [1102.2357].

[54] B. Allanach, *Impact of CMS Multi-jets and Missing Energy Search on CMSSM Fits*, *Phys.Rev.* **D83** (2011) 095019 [1102.3149].

[55] F. Feroz and M. P. Hobson, *Multimodal nested sampling: an efficient and robust alternative to MCMC methods for astronomical data analysis*, *Mon. Not. Roy. Astron. Soc.* **384** (2008) 449–463 [0704.3704].

[56] J. Skilling, *Nested sampling*, in *Bayesian Inference and Maximum Entropy Methods in Science and Engineering* (R. P. R. Fischer and U. von Toussaint, eds.), vol. 735, pp. 395–405, 2004.

[57] J. Skilling, *Nested sampling for general bayesian computation*, *Bayesian Analysis* **1** (2006), no. 4 833–860.

[58] M. Cabrera, J. Casas and A. Delgado, *Upper Bounds on Superpartner Masses from Upper Bounds on the Higgs Boson Mass*, *Phys.Rev.Lett.* **108** (2012) 021802 [1108.3867].

[59] G. F. Giudice and A. Strumia, *Probing High-Scale and Split Supersymmetry with Higgs Mass Measurements*, *Nucl.Phys.* **B858** (2012) 63–83 [1108.6077].

[60] A. Collaboration, *Physics at a high-luminosity lhc with atlas*, Tech. Rep. ATL-PHYS-PUB-2012-001, CERN, Geneva, Aug, 2012.

[61] J. R. Ellis, G. Ridolfi and F. Zwirner, *Radiative corrections to the masses of supersymmetric Higgs bosons*, *Phys. Lett.* **B257** (1991) 83–91.

[62] J. R. Ellis, G. Ridolfi and F. Zwirner, *On radiative corrections to supersymmetric Higgs boson masses and their implications for LEP searches*, *Phys. Lett.* **B262** (1991) 477–484.

[63] Y. Okada, M. Yamaguchi and T. Yanagida, *Upper bound of the lightest Higgs boson mass in the minimal supersymmetric standard model*, *Prog. Theor. Phys.* **85** (1991) 1–6.

[64] Y. Okada, M. Yamaguchi and T. Yanagida, *Renormalization group analysis on the Higgs mass in the softly broken supersymmetric standard model*, *Phys. Lett.* **B262** (1991) 54–58.

[65] H. E. Haber and R. Hempfling, *Can the mass of the lightest Higgs boson of the minimal supersymmetric model be larger than m(Z)?*, *Phys. Rev. Lett.* **66** (1991) 1815–1818.

[66] R. Barbieri, M. Frigeni and F. Caravaglios, *The Supersymmetric Higgs for heavy superpartners*, *Phys. Lett.* **B258** (1991) 167–170.

[67] M. S. Carena, J. Espinosa, M. Quiros and C. Wagner, *Analytical expressions for radiatively corrected Higgs masses and couplings in the MSSM*, *Phys.Lett.* **B355** (1995) 209–221 [hep-ph/9504316].

[68] L. Aparicio, D. Cerdeno and L. Ibanez, *A 119-125 GeV Higgs from a string derived slice of the CMSSM*, *JHEP* **1204** (2012) 126 [1202.0822].

[69] G. Jungman, M. Kamionkowski and K. Griest, *Supersymmetric dark matter*, *Phys.Rept.* **267** (1996) 195–373 [hep-ph/9506380].

[70] L. Knox and M. S. Turner, *Inflation at the electroweak scale*, *Phys.Rev.Lett.* **70** (1993) 371–374 [astro-ph/9209006].

[71] A. Ibarra and D. Tran, *Decaying Dark Matter and the PAMELA Anomaly*, *JCAP* **0902** (2009) 021 [0811.1555].

[72] M. Pato, L. Baudis, G. Bertone, R. Ruiz de Austri, L. E. Strigari *et. al.*, *Complementarity of Dark Matter Direct Detection Targets*, *Phys.Rev.* **D83** (2011) 083505 [1012.3458].

[73] J. R. Ellis, K. A. Olive and C. Savage, *Hadronic Uncertainties in the Elastic Scattering of Supersymmetric Dark Matter*, *Phys.Rev.* **D77** (2008) 065026 [0801.3656].

[74] G. Bertone, D. G. Cerdeno, M. Fornasa, R. Ruiz de Austri, C. Strege *et. al.*, *Global fits of the cMSSM including the first LHC and XENON100 data*, *JCAP* **1201** (2012) 015 [1107.1715].

[75] N. Arkani-Hamed, A. Delgado and G. Giudice, *The Well-tempered neutralino*, *Nucl.Phys.* **B741** (2006) 108–130 [hep-ph/0601041].

[76] G. Bertone, K. Kong, R. R. de Austri and R. Trotta, *Global fits of the Minimal Universal Extra Dimensions scenario*, *Phys.Rev.* **D83** (2011) 036008 [1010.2023].

[77] G. Bertone, D. G. Cerdeno, M. Fornasa, R. R. de Austri and R. Trotta, *Identification of Dark Matter particles with LHC and direct detection data*, *Phys.Rev.* **D82** (2010) 055008 [1005.4280].

[78] M. Davier, A. Hoecker, B. Malaescu, C. Z. Yuan and Z. Zhang, *Reevaluation of the hadronic contribution to the muon magnetic anomaly using new e+e- → pi+pi- cross section data from BABAR*, *Eur. Phys. J.* **C66** (2010) 1–9 [0908.4300].

[79] M. Davier *et. al.*, *The Discrepancy Between tau and e+e- Spectral Functions Revisited and the Consequences for the Muon Magnetic Anomaly*, *Eur. Phys. J.* **C66** (2010) 127–136 [0906.5443].

[80] G. Degrassi and G. Giudice, *QED logarithms in the electroweak corrections to the muon anomalous magnetic moment*, *Phys.Rev.* **D58** (1998) 053007 [hep-ph/9803384].

[81] S. Heinemeyer, D. Stockinger and G. Weiglein, *Two loop SUSY corrections to the anomalous magnetic moment of the muon*, *Nucl.Phys.* **B690** (2004) 62–80 [hep-ph/0312264].

[82] S. Heinemeyer, D. Stockinger and G. Weiglein, *Electroweak and supersymmetric two-loop corrections to (g-2)(mu)*, *Nucl.Phys.* **B699** (2004) 103–123 [hep-ph/0405255].

[83] S. Marchetti, S. Mertens, U. Nierste and D. Stockinger, *Tan(beta)-enhanced supersymmetric corrections to the anomalous magnetic moment of the muon*, *Phys.Rev.* **D79** (2009) 013010 [0808.1530].

[84] P. von Weitershausen, M. Schafer, H. Stockinger-Kim and D. Stockinger, *Photonic SUSY Two-Loop Corrections to the Muon Magnetic Moment*, *Phys.Rev.* **D81** (2010) 093004 [1003.5820].

[85] R. Trotta, *Applications of Bayesian model selection to cosmological parameters*, *Mon. Not. Roy. Astron. Soc.* **378** (2007) 72–82 [astro-ph/0504022].

[86] R. Trotta, *Bayes in the sky: Bayesian inference and model selection in cosmology*, *Contemp. Phys.* **49** (2008) 71–104 [0803.4089].

[87] F. Feroz, M. P. Hobson, L. Roszkowski, R. Ruiz de Austri and R. Trotta, *Are $BR(b \to s\gamma)$ and $(g-2)_\mu$ consistent within the Constrained MSSM?*, 0903.2487.

[88] M. E. Cabrera, J. Casas, R. R. de Austri and R. Trotta, *Quantifying the tension between the Higgs mass and $(g-2)_\mu$ in the CMSSM*, 1011.5935.

[89] B. de Carlos and J. Casas, *One loop analysis of the electroweak breaking in supersymmetric models and the fine tuning problem*, *Phys.Lett.* **B309** (1993) 320–328 [hep-ph/9303291].

[90] G. W. Anderson and D. J. Castano, *Measures of fine tuning*, *Phys.Lett.* **B347** (1995) 300–308 [hep-ph/9409419].

[91] P. Ciafaloni and A. Strumia, *Naturalness upper bounds on gauge mediated soft terms*, *Nucl.Phys.* **B494** (1997) 41–53 [hep-ph/9611204].

[92] L. Giusti, A. Romanino and A. Strumia, *Natural ranges of supersymmetric signals*, *Nucl.Phys.* **B550** (1999) 3–31 [hep-ph/9811386].

[93] J. Casas, J. Espinosa and I. Hidalgo, *Implications for new physics from fine-tuning arguments. 1. Application to SUSY and seesaw cases*, *JHEP* **0411** (2004) 057 [hep-ph/0410298].

[94] J. Casas, J. R. Espinosa and I. Hidalgo, *Implications for new physics from fine-tuning arguments. II. Little Higgs models*, *JHEP* **0503** (2005) 038 [hep-ph/0502066].

[95] B. Allanach, *Naturalness priors and fits to the constrained minimal supersymmetric standard model*, *Phys.Lett.* **B635** (2006) 123–130 [hep-ph/0601089].

[96] P. Athron and . Miller, D.J., *A New Measure of Fine Tuning*, *Phys.Rev.* **D76** (2007) 075010 [0705.2241].

[97] S. Fichet, *Quantified naturalness from Bayesian statistics*, 1204.4940.

[98] D. Ghilencea and G. Ross, *The fine-tuning cost of the likelihood in SUSY models*, *Nucl.Phys.* **B868** (2013) 65–74 [1208.0837].

[99] S. P. Martin, *Compressed supersymmetry and natural neutralino dark matter from top squark-mediated annihilation to top quarks*, *Phys.Rev.* **D75** (2007) 115005 [hep-ph/0703097].

[100] J. L. Feng, K. T. Matchev and T. Moroi, *Multi - TeV scalars are natural in minimal supergravity*, *Phys.Rev.Lett.* **84** (2000) 2322–2325 [hep-ph/9908309].